ELSEVIER

EXPERIMENTAL HEMATOLOGY

Experimental Hematology 31 (2003) 789–797

Functional CD5$^+$ B cells develop predominantly in the spleen of NOD/SCID/γc^{null} (NOG) mice transplanted either with human umbilical cord blood, bone marrow, or mobilized peripheral blood CD34$^+$ cells

Takuya Matsumura[a,b], Yoshie Kametani[b], Kiyoshi Ando[c], Yasuyuki Hirano[b], Ikumi Katano[b], Ryoji Ito[b,g], Masashi Shiina[b], Hideo Tsukamoto[d], Yuki Saito[e], Yutaka Tokuda[e], Shunichi Kato[f], Mamoru Ito[g], Kazuo Motoyoshi[a], and Sonoko Habu[b]

[a]*Third Department of Internal Medicine, National Defense Medical College, Saitama, Japan; Departments of* [b]*Immunology,* [c]*Hematology & Oncology,* [e]*Surgery, and* [f]*Pediatrics, Tokai University School of Medicine, Kanagawa, Japan;* [d]*Laboratory for Molecular Science Research, Tokai University School of Medicine, Kanagawa, Japan; and* [g]*Central Institute for Experimental Animals, Kanagawa, Japan*

(Received 10 January 2003; revised 5 April 2003; accepted 10 June 2003)

Objective. **Human CD5$^+$ B cells are the major B cell subset in fetal spleen and umbilical cord blood (CB), and their number gradually diminishes in both spleen and peripheral blood from infancy through childhood while conventional B cells increase. In this study, we investigated whether CD5$^+$ cells differentiate from adult hematopoietic stem cells (HSCs) as well as fetal ones in immunodeficient mice.**

Methods. **In our system, NOD/SCID/γc^{null} (NOG) mice were transplanted with CD34$^+$ cells from CB (hCB model), adult bone marrow (hBM model), and mobilized peripheral blood (hMPB model).**

Results. **In these model mice, a high proportion of CD19$^+$IgM$^+$CD5$^+$ mature B cells appeared in the spleen, regardless of the CD34$^+$ cell origin, 4 to 8 weeks after transplantation, while the majority were CD19$^+$IgM$^-$CD5$^-$ immature B cells in BM. The CD19$^+$CD5$^-$ BM cells showed to express CD5 after the coculture with NOG spleen cells. In the sera of immunized hCB model mice with DNP-KLH, antigen-specific IgM but not IgG was enhanced.**

Conclusion. **Our results show that adult CD34$^+$ cells develop into functional CD5$^+$ B cells in NOG spleen as much as fetal CD34$^+$ cells do.** © **2003 International Society for Experimental Hematology. Published by Elsevier Inc.**

Xenotransplantation using nonobese diabetic/severe combined immunodeficient (NOD/SCID) mice [1,2] has been widely used in the investigation of human hematopoietic stem cells (HSCs). Multilineage differentiation and self-renewal ability of human CD34$^+$ cells have been shown in this model [3–9]. Especially, human B cells are abundantly generated in NOD/SCID mice transplanted with human CD34$^+$ cells [9]. This model appears to provide a promising in vivo system to study the development and maturation of human B cells.

Human and murine B cells are composed of B1 and B2 cell subsets and the expression of CD5 has been used to distinguish B-1a cells, the major subset of B-1 cells [10,11]. CD5$^+$ B1 cells are different from conventional CD5$^-$ B2 cells with respect to anatomic localization [12], gene usage [13], and function [13,14]. Moreover, CD5$^+$ B1 cells are known to produce natural antibodies, mostly IgM, and play an important role in early innate defense systems. In human beings, CD5$^+$ B1 cells are present predominantly in the fetal spleen and umbilical cord blood; those cells reduce gradually with age and represent only 10 to 20% of adult peripheral B cells. However, CD5$^+$ B cells are reported to increase in certain types of autoimmune disorders.

The origin of CD5$^+$ B1 cells is still poorly understood. The relationship between precursors for CD5$^+$ B1 cells and CD5$^-$ B2 cells remains controversial. There are ontogeny-related differences in the developmental potential of B1 and B2 subsets. Mouse fetal liver cells differentiate into both B1 and B2 cells while adult bone marrow (BM) cells differentiate into only B2 cells after transplantation [15].

Offprint requests to: Sonoko Habu, M.D., Boseidai, Isehara, Kanagawa, 259-1193 Japan; E-mail: sonoko@is.icc.u-tokai.ac.jp

0301-472X/03 $-see front matter.
doi: 10.1016/S0301-472X(03)00193-0

Therefore, in mice, $CD5^+$ B1 cells derive from fetal liver HSCs, but not from adult HSCs, and self-replenish throughout life.

In clinical stem cell transplantation of human patients, appearance of $CD5^+$ B cells has been reported in both cases of HSC from BM and umbilical cord blood (CB) cells, respectively [16,17]. Novelli et al. showed the similar result of xenogeneic combination in which human $CD34^+$ BM cells develop in NOD/SCID mice [18]. They also examined the appearance of $CD5^+$ B cells from CB cells but did not compare with that of BM cells because of the low frequency of the engraftment in the mice.

Recently, we generated NOD/SCID/γc^{null} (NOG) mice, which are double homozygous for the severe combined immunodeficiency (SCID) mutation and interleukin-2Rγ (IL-2Rγ) allelic mutation (γc^{null}), and showed high levels of engraftment of human blood cells and multilineage differentiation including mature T and B cells from CB $CD34^+$ cells [19–21]. These mutant mice made it possible to compare the developmental difference of $CD5^+$ B cells from human adult and fetal origin of HSC in transplanted animals. In this study, we investigated the ontogenic difference of B cell subset differentiation from human HSC using NOG mice transplanted with hCB, hBM, and hMPB $CD34^+$ cells. Surprisingly, functional $CD5^+$ B cells developed after transplantation not only with hCB but also with adult hBM or hMPB $CD34^+$ cells. We also showed that the spleen, but not BM, of NOG mice provides the environment for the development of human $CD5^+$ B cells.

Materials and methods

Mice

NOD/Shi-scid, common γc^{null} (NOD/SCID/γc^{null}; NOG) mice were provided from the Central Institute for Experimental Animals (Kawasaki, Japan). All mice were kept under specific pathogen-free conditions in the animal faculty located at the Tokai University School of Medicine (Isehara, Japan).

Human hematopoietic stem cells

Human umbilical cord blood (hCB) was obtained from full-term healthy newborns immediately after vaginal delivery. Human bone marrow (hBM) was collected from healthy adults. Human mobilized peripheral blood (hMPB) was harvested from healthy adults for allogeneic transplantation or patients of malignant lymphoma during complete remission for autologous transplantation. Informed consents were obtained according to the Institute guidelines, and this work was approved by Tokai University Human Research Committee. Mononuclear cells (MNC) were separated by Ficoll-Paque PLUS (Amersham Biosciences, Piscataway, NJ, USA) density-gradient centrifugation. $CD34^+$ cells were purified from MNC using the 2-step of MACS system (Miltenyi Biotec, Gladbach, Germany). The purity of $CD34^+$ cells was 98.3% ± 2.4%. In some experiments, $CD34^+$ cells were serially purified using MACS system and FACS Vantage to prevent a contamination of T cells and $CD34^+CD19^+$ cells. The purity of $CD34^+$ cell fraction was 99.4% ± 0.8%.

Transplantation

Nine-week-old NOG mice were irradiated sublethally with 250 cGy prior to the transplantation and $CD34^+$ cells were transplanted intravenously. From 4 weeks after transplantation, the peripheral blood was obtained every 2 weeks via orbit under inhalation anesthesia. Mice were sacrificed 14 weeks after transplantation and the lymphoid organs were used for analysis.

Monoclonal antibodies, flow cytometry, and cell sorting

All cells were analyzed using FACS Calibur (Becton Dickinson, Franklin Lakes, NJ, USA). For each analysis or sorting, living gate white blood cells or lymphocytes were further gated on human $CD45^+$ cells. Mouse anti-human monoclonal antibodies (mAbs) are listed below: fluorescein isothiocyanate (FITC)-conjugated CD3, CD4, CD5, CD20, CD34, IgM, κ-chain; phycoerythrin (PE)-conjugated CD4, CD5, CD8, CD10, CD19, IgD, λ-chain; PerCP-conjugated CD45; APC-conjugated CD19 from Becton Dickinson PharMingen (San Jose, CA, USA).

In vitro coculture system

Mice were sacrificed 14 weeks after transplantation and the BM cells were sorted into $CD19^+IgM^-CD5^-$ cells. Spleen stroma cells were prepared from irradiated 9-week-old NOG mice by trypsin treatment and plated into 96-well plates (Becton Dickinson). These stroma cell suspensions contained no mouse lymphocytes. Bone marrow stroma cells were prepared from 9-week-old mice after irradiation as mentioned above without trypsin treatment. These cells also contained no mouse lymphocytes. Sorted $CD19^+$ IgM^-CD5^- cells were transferred onto spleen or BM cells at a concentration of 8.0×10^4 cells/well and incubated at 37°C in a humidified atmosphere containing 5% CO_2. Cultured cells were harvested after 1 or 2 weeks and analyzed as described above.

Immunization and ELISA

Inducing antibody response, some mice were immunized intraperitoneally with 100 μg of 2.4-dinitrophenol-conjugated keyhole-limpet-hemocyanin (DNP-KLH) in normal saline from 4 weeks after transplantation with hCB, hBM, and hMPB $CD34^+$ cells and boosted every 2 weeks until sacrificing the mice. Enzyme-linked immunosorbent assay (ELISA) for human IgG and IgM production was performed as described previously [19].

Statistical analysis

Statistical analysis was done with Microsoft Excel (Microsoft, Redmond, WA, USA) and StatView (SAS Institute, Cary, NC, USA). Data were represented as mean value ± standard deviation (SD). Significant differences between data groups were determined by two-sided Student's *t*-test analysis.

Results

High engraftment of human $CD34^+$ cells derived from adult and cord blood in NOG mice

The engraftment efficiency of human $CD34^+$ cells from different tissues was compared in NOG mice. As the source of human $CD34^+$ cells, we used umbilical cord blood (hCB), bone marrow (hCB), and mobilized peripheral blood (hMPB), and the purity of $CD34^+$ cells was more than 98%. The recipient NOG mice receiving $CD34^+$ cells from hCB,

Table 1. Comparison of human blood cell engraftment in hCB, hBM, and hMPB models

Exp. number	No. of injected $CD34^+$ cells $n \times 10^5$	Origin of $hCD34^+$ cells	Unique number of samples	% of $CD34^+CD19^+$ cells	In the transplanted NOG mice: No. of total cells BM $n \times 10^7$	Sp $n \times 10^6$	PB $n \times 10^4$	% of $hCD45^+$ cells BM %	Sp %	PB %	No. of $hCD45^+$ cells BM $n \times 10^7$	Sp $n \times 10^6$	PB $n \times 10^4$
1	1.8	hCB	1	3.3	2.7	11.0	18.0	52.8	29.8	32.3	1.4	3.3	5.8
2	5.6	hCB	2	1.5	1.6	26.0	12.0	62.9	13.2	78.0	1.0	3.4	9.4
3	4.7	hCB	3	4.4	1.8	3.4	20.0	22.4	78.4	7.6	0.4	2.7	1.5
4	4.0	hCB	4	5.2	2.9	16.0	4.0	93.3	86.6	90.1	2.7	13.9	3.6
5	4.0	hCB	5	1.7	2.4	11.0	7.0	86.3	55.9	74.0	2.1	6.1	5.2
6	2.7	hCB	6	0.0	4.1	19.0	30.0	84.2	89.3	5.8	3.5	17.0	1.7
7	4.0	hCB	7	0.0*	2.3	24.0	14.0	88.5	84.1	90.8	2.0	20.2	12.7
8	3.0	hCB	8	0.0*	1.8	4.1	94.0	43.5	72.5	1.1	0.8	3.0	1.0
average	3.7			2.0*	2.5	14.3	24.9	66.7	63.7	47.5	1.7	8.7	5.1
SD	1.2			2.1	0.8	8.5	29.1	25.6	28.4	39.7	1.0	7.2	4.1
9	1.9	hBM	9	9.8	1.5	5.0	3.0	57.3	8.1	14.8	0.9	0.4	0.4
10	3.6	hBM	10	72.3	1.6	3.5	3.8	4.7	0.9	0.5	0.1	0.0	0.0
11	3.5	hBM	11	51.9	1.7	5.2	16.0	6.0	1.8	1.3	0.1	0.1	0.2
12	3.6	hBM	12	49.1	1.6	5.9	7.8	23.7	3.6	5.9	0.4	0.2	0.5
13	14.0	hBM	13	37.5	1.5	3.1	47.0	31.7	66.0	18.1	0.5	2.0	8.5
14	2.8	hBM	14	0.0	1.8	1.8	2.5	11.7	3.6	8.1	0.2	0.1	0.2
average	4.9			36.8	1.6	4.1	13.4	22.5†	14.0†	8.1†	0.4†	0.5†	1.6
SD	4.5			27.3	0.1	1.5	17.2	20.0	25.6	7.1	0.3	0.8	3.4
15	18.0	hMPB	15	7.8	1.7	9.1	16.0	71.3	16.3	9.8	1.2	1.5	1.6
16	16.5	hMPB	16	0.1	2.7	5.4	2.0	30.4	4.5	3.6	0.8	0.2	0.1
17	16.5	hMPB	16	0.1	3.2	4.4	5.3	46.4	31.3	17.9	1.5	1.4	0.9
18	5.0	hMPB	17	0.1	1.6	1.7	4.5	59.1	19.3	17.8	0.9	0.3	0.8
19	5.0	hMPB	17	0.1	2.6	5.8	3.8	27.1	2.4	3.3	0.7	0.1	0.1
20	9.0	hMPB	18	0.0*	2.0	7.9	30.0	37.3	2.0	8.1	0.7	0.2	2.4
21	9.0	hMPB	18	0.0*	2.7	4.0	8.8	50.3	28.4	15.1	1.4	1.1	1.3
22	5.0	hMPB	19	0.0*	1.9	5.3	11.0	41.2	5.9	10.3	0.8	0.3	1.1
average	10.5			1.0	2.3	5.5	10.2	45.4†	13.8†	10.7†	1.0†	0.6†	1.1†
SD	5.7			2.7	0.6	2.3	9.2	14.8	11.8	5.8	0.3	0.6	0.8

Human engraftments of hCB, hBM, and hMPB models were compared. The number of total cells, the percentage of human $CD45^+$ cells, and the number of human $CD45^+$ cells in BM, spleen, and PB of these models were determined by flow cytometry 14 wks after transplantation. Number of mice: in hCB, n = 8; in hBM, n = 6; in hMPB, n = 8.

*In some experiments, sorted $CD34^+$ cells were injected.

†Differences between hCB and either hBM or hMPB models were statistically significant in the BM, spleen, and PB of NOG mice ($p < 0.05$).

hBM, and hMBP were termed as hCB, hBM, and hMBP model, respectively. Fourteen weeks after transplantation, all mouse models were found to be highly chimeric for human $CD45^+$ cells (Table 1). Among them, human $CD45^+$ cells showed significantly higher proportion and number in the hCB model than that in hBM or hMPB model in BM, spleen, or peripheral blood (PB) of NOG mice.

In NOG BM, the human $CD45^+$ cells were composed of major populations of $CD19^+$ B cells (~70%), a relatively small proportion of $CD33^+$ myeloid cells (~10%), and a few $CD3^+$ T cells (~1%) in all three models (Table 2A).

We have already reported that human-derived $CD4^+$ and/or $CD8^+$ cells were detected in the thymi of hCB model mice [20,21]. In this study, the frequency of human T cells in the thymus was compared in three model systems (Table 2B). The number of mice which contained human $CD45^+$ cells in the thymi was 6 in 7 in the hCB model, 2 in 6 in the hBM model, and 4 in 6 in the hMPB model. The proportions of CD4/CD8 double-positive (DP) and CD4 or CD8 single-positive (SP) T cells were similar to that of normal human thymocytes.

Appearance of $CD5^+$ B cell subset in the spleen of all three model mice

In NOG spleen, the majority of human $CD45^+$ cells expressed CD19 in all three models (Fig. 1). More than 50% of $CD19^+$ cells in spleen and PB expressed CD5 in all three model mice 14 weeks after the transplantation (Table 3 and Fig. 1). In addition to CD5, $CD19^+$ cells also expressed IgM and CD20 (Table 3 and Fig. 2A and C), and most of spleen IgM^+ cells were IgD^+ (Fig. 2B). Moreover, $CD5^+IgM^+$ cells mostly expressed both IgM and IgD. Based on these phenotypes, most of $CD19^+CD5^+$ cells in the spleen and PB are suggested to be in the mature B cell stage. In contrast, NOG BM contained few $CD19^+$ cells expressing CD5 or CD20, and both $CD19^+CD5^+$ cells and $CD19^+CD5^-$ cells in NOG BM were almost all IgM^-IgD^- cells, indicating that $CD19^+$ BM cells were immature.

Table 2. Multi-lineage differentiation of human blood cells in the bone marrow of hCB, hBM, and hMPB models

	hCB	hBM	hMPB
Origin of injected $CD34^+$ cells*			
$CD19^+$	74.23 ± 16.44	75.44 ± 12.88	79.11 ± 4.72
$CD33^+$	13.80 ± 7.93	7.29 ± 4.59	10.26 ± 3.02
$CD3^+$	1.25 ± 1.49	0.30 ± 0.36	0.28 ± 0.11
Origin of injected $CD34^+$ cells†			
positive mice/ total mice	6/7	2/6	4/6
%DP	74.15	92.04	83.59
%CD4SP	12.40	1.85	5.49
%CD8SP	11.89	3.85	6.92
$\%CD19^+$	0.78	2.03	3.30

*Multi-lineage differentiation of human blood cells was examined in the BM of either hCB, hBM, or hMPB models 14 weeks after transplantation. For each analysis, cells were gated within the live white blood cells and human $CD45^+$ cells. The percentage of human cells expressing each antigen was determined by flow cytometry. Data are represented as the mean value ± SD. Number of mice: in hCB, n = 7; in hBM, n = 6; in hMPB, n = 6.

†Lymphopoiesis was examined in the thymus of hCB, hBM, and hMPB models 14 weeks after the transplantation. For each analysis, cells were gated within the live lymphocyte, and moreover gated on human $CD45^+$ cells. Mice were determined as positive if lumphopoiesis was detectable in the thymus. %DP, %CD4SP, %CD8SP, and %CD19 are the percentage of human cells expressing the antigen of $CD4^+CD8^+$, $CD4^+CD8^-$, $CD4^-CD8^+$, and $CD19^+$ determined by flow cytometry, respectively. Data are represented as the mean value.

$CD5^+$ B1 cells are known to be localized predominantly within the peritoneal cavity in mice. However, a very few $CD45^+$ cells, including $CD19^+CD5^+$ cells, were found in peritoneal cavities of all three modes (data not shown). Since human umbilical cord blood cells are known to contain $CD5^+$ B cells, we compared the expression profiles of human B cells between the fresh cord blood (fCB) and

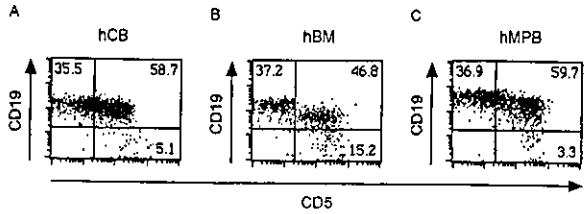

Figure 1. $CD5^+$ cells are dominant in the spleen of hCB, hBM, and hMPB models. Human $CD45^+$ cells in the spleens of NOG mice 14 weeks after transplantation were analyzed for B cell markers (CD19 and CD5) by flow cytometry. Representative data from either hCB (A), hBM (B), or hMPB (C) models were shown in the $CD45^+$ cell gates. Numbers in the plots indicate the percentages of human $CD45^+$ cells.

$CD19^+CD5^+$ cells in PB of hCB model mice to see if these cells shared the same character. $CD19^+$ cells in NOG spleen and PB expressed IgM, CD5, IgD, and CD20 at the levels similar to those found in fCB B cells (Fig. 2C).

These results showed that $CD5^+$ mature B cells were dominant in the spleen and PB of all three models and the expression of surface molecules were closely related to fCB $CD5^+$ B cells.

Increase of human $CD5^+$ B cells in the periphery of NOG mice following transplantation

As $CD19^+CD5^+$ cells were largely detectable in the spleen and PB of NOG mice, the appearance of $CD19^+CD5^+$ cells was examined in the spleen of hCB model mice serially at 3, 4, 5, and 8 weeks after transplantation. As shown in Figure 3, the frequency of $CD5^+$ cells in $CD19^+$ cells was around 15% at week 4 and increased gradually in the spleen, reaching a plateau between 8 and 14 weeks after transplantation (Fig. 3B and D). IgM^+ cells in $CD19^+$ cells also increased in correlation with $CD5^+$ cells (Fig. 3C). In BM, however, $CD19^+$ cells were almost $CD5^-$ and contained a small proportion of IgM^+ cells until 8 to 14 weeks after

Table 3. B cell subsets in the bone marrow, spleen, and peripheral blood of hCB, hBM, and hMPB model mice

Organ in NOG mice	BM			Spleen			PB		
Origin of injected $CD34^+$ cells	hCB	hBM	hMPB	hCB	hBM	hMPB	hCB	hBM	hMPB
In $CD45^+$ cells									
$CD19^+$	96.5 ± 2.1	98.4 ± 0.5	98.6 ± 1.1	86.1 ± 11.8	92.4 ± 2.8	91.9 ± 3.2	70.2 ± 22.2	82.3 ± 14.2	72.4 ± 12.5
$CD34^+$	7.1 ± 4.8	3.7 ± 2.8	1.2 ± 0.9*	n.d.	n.d.	n.d.	n.d.	n.d.	n.d.
kappa/lambda	0.4 ± 0.1	0.4 ± 0.1	0.3 ± 0.1	0.8 ± 0.2	0.8 ± 0.2	1.1 ± 0.3	n.d.	n.d.	n.d.
In $CD19^+$ cells									
$CD5^+$	3.0 ± 1.8	4.1 ± 2.1	2.1 ± 0.6	61.8 ± 17.6	63.4 ± 9.5	72.5 ± 10.1	76.4 ± 10.7	77.6 ± 13.7	75.3 ± 18.0
IgM^+	18.4 ± 3.8	14.9 ± 3.6	11.6 ± 2.2	76.3 ± 14.9	62.6 ± 11.7	71.5 ± 8.8	84.6 ± 7.8	85.2 ± 5.8	83.4 ± 7.8
IgG^+	0.2 ± 0.1	0.3 ± 0.3	0.1 ± 0.2	1.2 ± 1.1	2.1 ± 1.3	1.4 ± 1.2	n.d.	n.d.	n.d.
$CD20^+$	20.3 ± 15.2	18.6 ± 12.2	24.9 ± 9.3	76.5 ± 20.6	71.6 ± 19.6	83.0 ± 19.0	n.d.	n.d.	n.d.
In IgM^+ cells									
IgD^+	32.5 ± 11.3	25.1 ± 11.3	20.1 ± 5.4	83.9 ± 12.0	82.0 ± 10.3	79.9 ± 8.1	n.d.	n.d.	n.d.

Human B cell subsets were compared in the BM, spleen, and PB of hCB, hBM, and hMPB models 14 weeks after transplantation. For each analysis, cell gates are limited within the live lymphocyte of human $CD45^+$ cells. Values are the percentage of human cells expressing each antigen determined by flow cytometry. Data are represented as the means value ± SD. n.d. = not done. Number of mice: in hCB, n = 8; in hBM, n = 6; in hMPB, n = 7.

*Indicates significant difference from the percentages of surface marker in hCB model mice ($p < 0.05$).

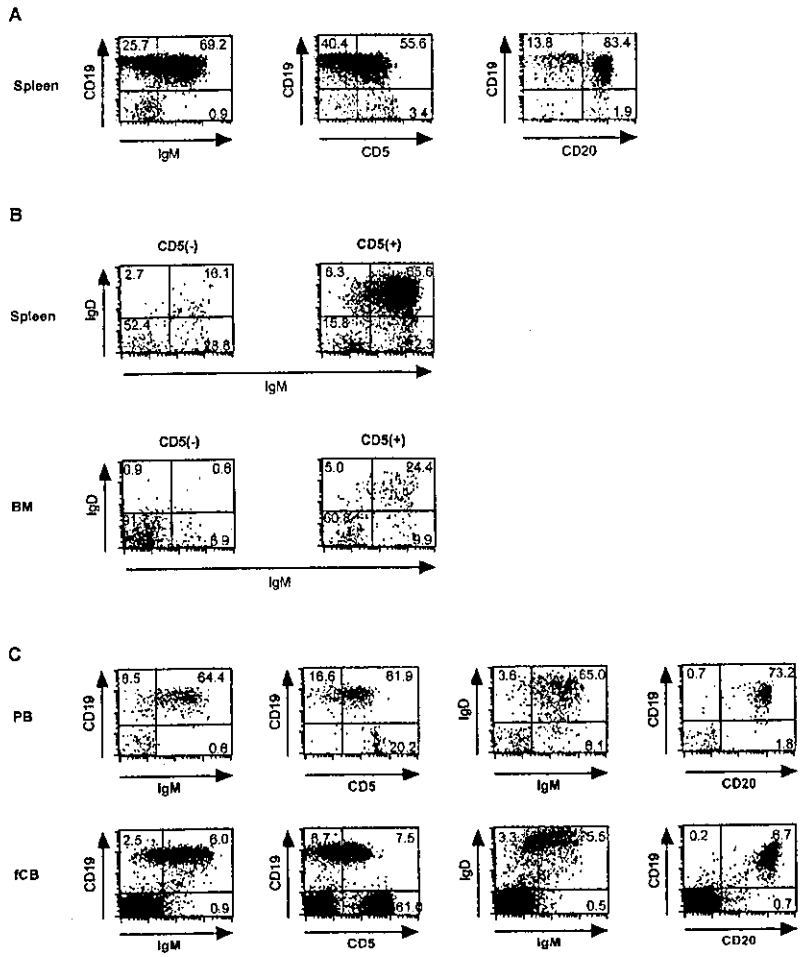

Figure 2. Human B cells developed in NOG express similar levels of B cell markers to human CB B cells. Flow cytometric analyses of $CD19^+$ cells were performed for B cell markers (IgM, CD5, and CD20) of spleen cells and BM cells in hCB model (**A**). $CD19^+CD5^+$ cells and $CD19^+CD5^-$ cells were analyzed for IgM and IgD expressions (**B**). The expression of B cell markers was analyzed for PB cells of hCB model and fCB (**C**). FACS analyses were performed for the mice 14 weeks after transplantation in the $CD45^+$ cell gate. Plots were from representative experiments shown in Table 3 (fCB, n = 3). Numbers in the plots indicate the percentages of human $CD45^+$ cells.

transplantation despite the presence of large numbers of $CD19^+$ cells.

The kinetics of $CD19^+IgM^+$ cells and IgM^+CD5^+ cells in PB was also examined in the hCB, hBM, and hMPB models (Fig. 4). The frequency of both cells increased gradually between 6 and 8 weeks after transplantation and reached a plateau between 8 and 12 weeks after transplantation without different frequency among three models. This kinetics pattern was similar to $CD5^+$ cells in the spleen. In estimation of both $CD19^+IgM^+$ and IgM^+CD5^+ cells, $CD5^+$ cells are more than 60% of $CD19^+$ cells.

These data suggested that the human $CD19^+CD5^+$ cells may develop in the NOG spleen environment and may circulate in PB. To determine whether immature $CD19^+$ B cells develop into $CD5^+$ B cells in the spleen environment, $CD19^+IgM^-CD5^-$ cells isolated from the BM cells of hCB model mice were cocultured with the spleen cells of NOG mice without transplantation. A significant increase of $CD19^+CD5^+$ B cells was observed after 2 weeks (Fig. 5). A similar result was observed in the expression of IgM (data not shown). On the other hand, coculture of $CD19^+IgM^-CD5^-$ cells with NOG BM cells did not promote the development of $CD19^+CD5^+$ B cells, instead of cell death within 7 days (data not shown).

These in vivo and in vitro data allowed us to assume that $CD19^+IgM^-CD5^-$ immature cells differentiate from $CD34^+$ cells in the BM and migrate into the spleen, where they become $CD19^+IgM^+CD5^+$ cells. Alternatively, human $CD34^+$ cells directly migrate into the spleen to develop into $CD19^+CD5^+$ cells without passing through BM.

Human antibody production in NOG mice transplanted with hCB, hBM, and hMPC $CD34^+$ cells

$CD5^+$ B1 cells are well known as the major source producing natural antibodies, mostly IgM, and hard-to-produce antigen-specific IgG. To examine that human B cells developed

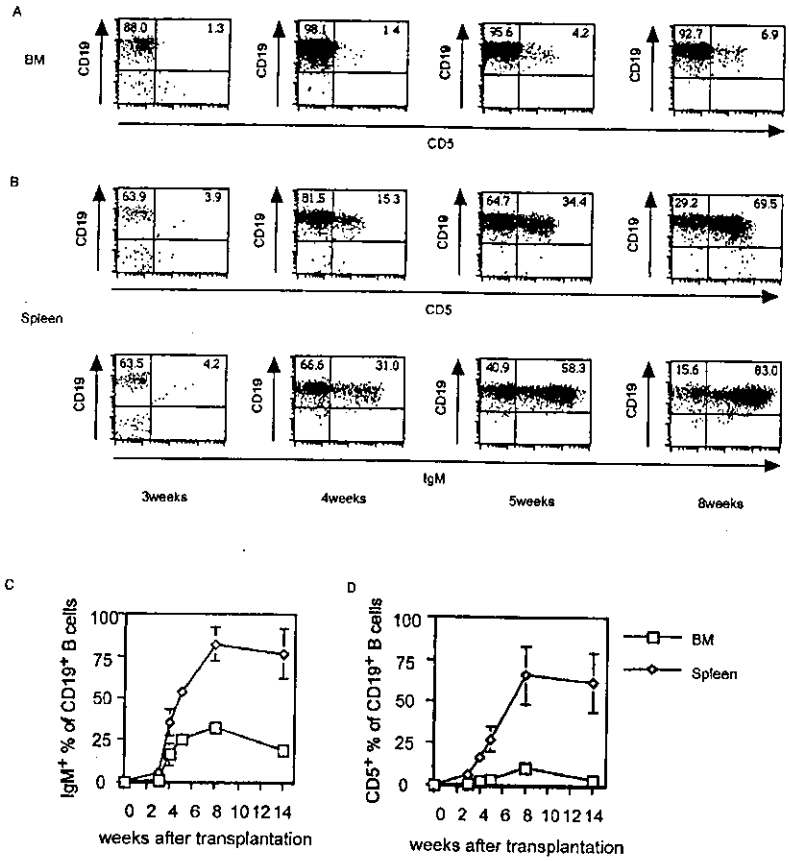

Figure 3. $CD5^+$ B cells accumulate in the NOG spleen of hCB model mice. Human B cell subsets in the BM (**A**) and spleen (**B**) of hCB model mice were analyzed by flow cytometry at 3, 4, 5, and 8 weeks after the transplantation. FACS profiles are from representative experiments (n = 3). Numbers in the plots indicates the percentages of human $CD45^+$ cells. Kinetics of the accumulation of $CD5^+$ cells (**C**) and IgM^+ cells (**D**) per $CD19^+$ cells were examined at 3, 4, 5, 8, and 14 weeks after $CD34^+$ cell transplantation. Human B cells in the bone marrow and spleen of hCB model mice were shown as open squares (BM) and open lozenges (spleen), respectively. Data were shown as the percentages of mean values (± SD). Number of mice used at each point was n = 3. In these experiments, $3.6 \pm 0.7 \times 10^5$ $CD34^+$ cells were injected, respectively.

in NOG mice have the ability to produce human antibodies upon antigen stimulation, three models were intraperitoneally immunized with DNP-KLH. The serum level of IgG and IgM was measured by ELISA for hCB, hBM, and hMPB models.

As shown in Figure 6, a significant increase of IgM concentrations was observed in the sera of these three models. The serum IgM produced by all immunized mice contained relative amounts of anti-DNP-KLH-specific IgM, and the production was enhanced by repeated stimulation. In contrast, antigen-specific IgG was not detected in any group of mice but only a small amount of nonspecific IgG was detected in hCB model (data not shown). As CD5-expressing cells were more than 60% of spleen $CD19^+$ cells (Fig. 3), antigen-specific IgM in the serum may be produced at least in part by $CD5^+$ B cells developed from human $CD34^+$ cells. We examined if the normal lymphoid architecture of the spleen of these models is reconstituted. The immunohistological study demonstrated the scattered presence of human $CD45^+$ and/or $CD20^+$ cells as well as a small number of $CD3^+$ T cells in the spleens of NOG mice. However, no follicular architecture was observed (data not shown). These results may implicate the absence or low IgG level of the serum in NOG mice receiving human $CD34^+$ cells.

Discussion

The CD5-expressing B cells are suggested to belong to the B1 subset. B1 and B2 subsets are distinguished by the expression of surface molecules, anatomic localization [12], gene usage [13], and function [13,14]; the major subset of B1 cells exists in a high proportion during fetal life and childhood, including in human umbilical cord blood, and few exist in adult bone marrow and peripheral blood [11]. However, little is characterized about the different potential of HSC between fetal and adult origins into B1 cells. In the present study, we demonstrated for the first time that human $CD34^+$ cells have an equivalent potential to develop into

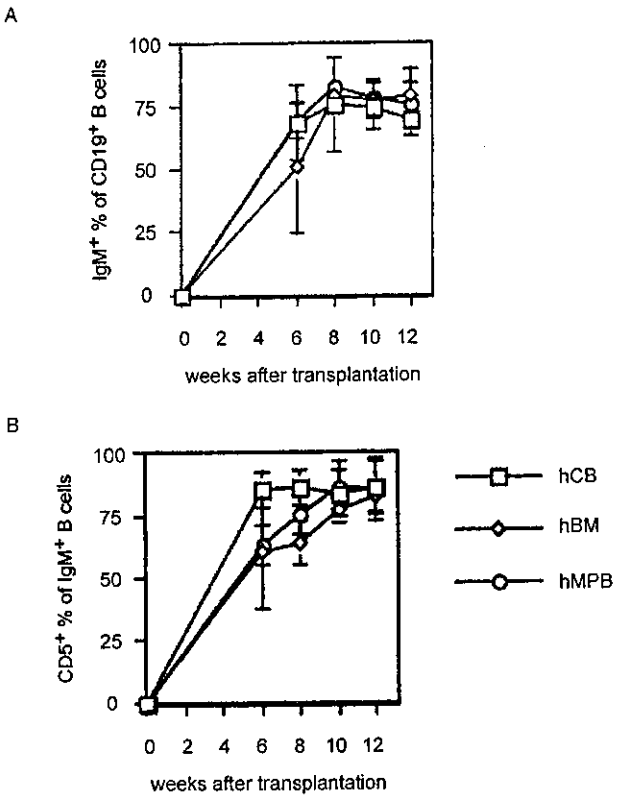

Figure 4. $CD5^+$ B cells circulate in the NOG mice transplanted with$CD34^+$ cells. Human B cell subsets in the PB of hCB (open squares), hBM (open lozenges), and hMPB (open circles) model mice were analyzed by flow cytometry at 6, 8, 10, and 12 weeks after transplantation. Data were shown as the percentages of mean values (± SD) of IgM cells per $CD19^+$ cells (**A**) or $CD5^+$ cells per IgM^+ cells (**B**). Number of mice used at each point was; hCB, n = 5, hBM, n = 4, hMPB, n = 5.

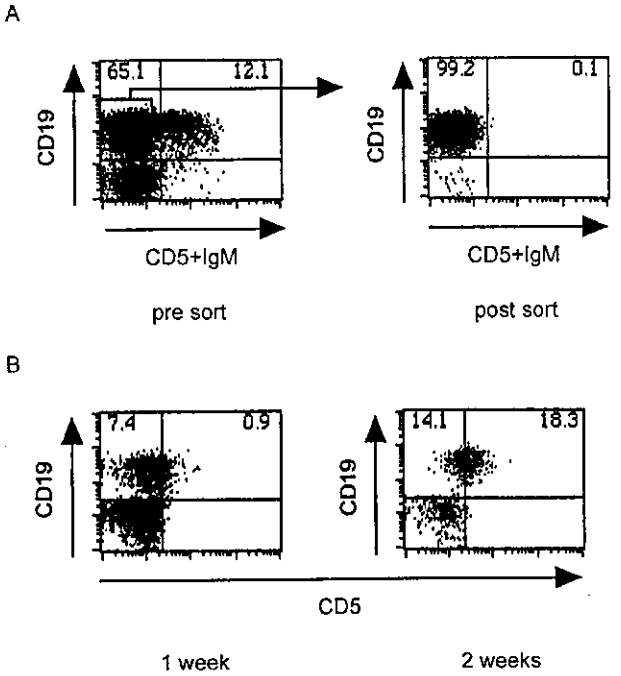

Figure 5. $CD5^+$ B cells develop in the coculture of immature B cells and NOG spleen cells. $CD19^+IgM^-CD5^-$ cells were collected from the bone marrow of hCB model mice 14 weeks after the transplantation. Sorting gate is shown in (**A**). The cells sorted according to the gate were cultured with the spleen cells of NOG mice, harvested 1 to 2 weeks later, and determined the appearance of $CD5^+$ B cells by flow cytometry. Numbers in the plots indicated the percentages of human $CD45^+$ cells. The cell number is 8.0×10^4 cells seeded and recovery after 1 week is 7.6×10^3, after 2 weeks 4.5×10^2.

$CD5^+$ B cells in any origins of the cord blood, bone marrow, and peripheral blood in the mouse environment.

To determine the developmental ability of human $CD34^+$ cells with different origins into $CD5^+$ cells, we generated mouse models using NOG mice reconstituted with human $CD34^+$ cells from CB, adult BM, and adult MPB, and compared developmental frequency of $CD5^+$ B cells. In these three models, the ratios of $CD19^+/CD45^+$ cells and $CD5^+/CD19^+$ cells in the spleen and PB were equivalently high, though the proportion of human $CD45^+$ cells was higher in the CB model than the BM and MPB models. In the BM of the three models, however, the proportion of $CD5^+$ B cells was low (less than 5%) and did not increase during 12 weeks posttransplantation, while the ratios of $CD5^+/CD19^+$ cells in PB increased gradually from 4 weeks after transplantation and reached up to 70% until the 12^{th} week. Instead of NOG mice, Navelli et al. used NOD/SCID mice receiving human CB cells and showed a high frequency of $CD5^+$ B cells in spleen but low in BM [18]. Recently, Wardemann et al. have reported that few $CD5^+$ B1 cells are found in the spleen of congenital Hox 11 defect mice and splenectomized wild mice [22]. Our in vitro experimental result showed sorted human $CD34^+$ cells become $CD5^+CD19^+$ cells (Fig. 5). Collectively, it is suggested that the splenic environment may possess a certain ability to induce $CD5^+$ B cells from any origin of HSC.

If $CD34^+$ cells derived from adult BM as well as CB have a potential to develop into $CD5^+$ B cells preferentially in the spleen, why are $CD5^+$ B cells so minor in the periphery of individuals in the physiological condition? The clinical studies showed that $CD5^+$ B cells increase transiently in the periphery of the patients after BM or CB transplantation and gradually decrease within several months with the increase of B2 cells ([16] and personal communication from M.R. Loken). In the mouse-mouse transplantation, it has been observed that $CD5^-$ B2 cells were the major population in the spleen of wild and NOG mice 12 weeks after transplantation of green fluorescent protein (GFP) mouse-derived $c\text{-}kit^+Lin^-$ BM cells ([23] and data not shown). These findings may bring a possible explanation that $CD5^+$ B cells can appear from the transplanted BM cells even in the allogeneic or syngeneic combination but are replaced by B2 cells, which may develop/proliferate later. This scenario is supported by our finding

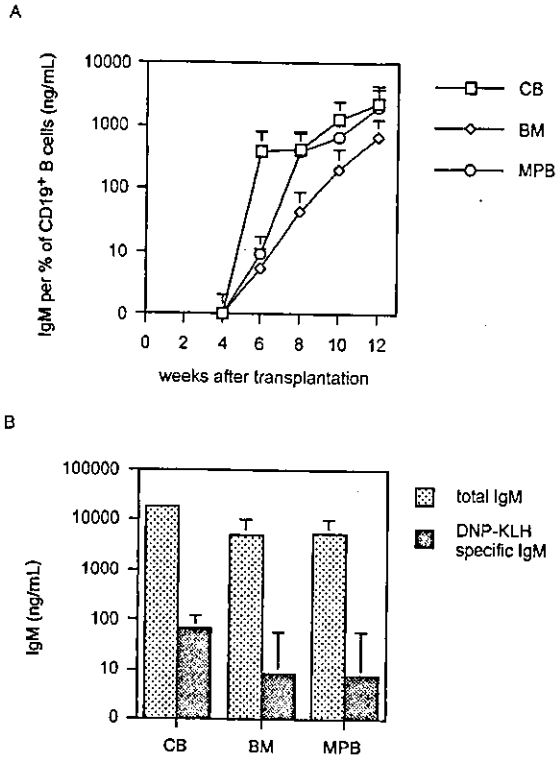

Figure 6. NOG mice transplanted with $CD34^+$ cells can produce antigen-specific IgM. The hCB, hBM, and hMPB model mice were immunized with DNP-KLH/alum every 2 weeks intraperitoneally from 4 weeks after transplantation. Spleen cells were stained with anti-CD19 and anti-IgM and analyzed by flow cytometry as shown in Figure 2C. The percentage of IgM^+ cells in $CD19^+$ cells were calculated from FACs patterns. Human immunoglobulin levels in the sera were measured by ELISA. **(A)** Mean values (± SD) of total IgM percentage of $CD19^+$ cells within the spleen were shown in the figure. The models are hCB (open squares), hBM (open lozenges), and hMPB (open circles), respectively. In each experiment, at least 4 mice were examined at each time point. **(B)** Each bar represents the mean value (± SD) of total IgM (dotted bars) and DNP-KLH-specific IgM (filled bars) at 12 weeks after $CD34^+$ cell transplantation.

that despite the high proportion of $CD5^+$ B cells in NOG spleen, their absolute cell number never increased but was almost equivalent to that of mouse $CD5^+$ B cells in wild mice or in NOG mice transplanted with mouse HSC (data not shown).

In the xenogeneic combination, however, several possibilities remain about the appearance of $CD5^+$ B cells; the mouse environment may not be sufficient for human $CD5^-$ B2 cell development in BM. For instance, mouse interleukin (IL)-7 cannot interact with human IL-7 receptor, though IL-7 is important for B2 cell development and survival. In fact, IL-7 targeting mice showed a B cell phenotype similar to our reconstituted NOG mice with human $CD34^+$ cells [24]. Other factors such as BAFF [25] and chemokine CXCL13 [26] involved in B2 cell development may also function in a species-specific manner. Identification of such factors may be important to clarify why $CD5^+$ B cells but not normal B2 cells preferentially develop in our system. It may also be indicated that a low level of human T-cell development causes a high appearance of $CD5^+$ B cells, as Novelli et al. suggested [18]. However, an equivalently high proportion of $CD5^+$B cells was detectable in the spleen of NOG mice, which possessed a high percentage of human T cells in the periphery (data not shown). Moreover, in the athymic nude mice, $CD5^+$ B cells were not increased (data not shown). Therefore, a high proportion of human $CD5^+$ B cells in NOG mice may be caused by the suppression of human B2 development in the xenogeneic environment with poorly developed T cells.

$CD5^+$B1 cells are known to be a major B cell subset in body cavities. In mice, $CD5^+$ B1 cells are very infrequent in the spleen and peripheral blood, but are predominant in the peritoneal cavity [12]. In our model mice, only a few human $CD5^+$ B cells were detectable in the peritoneal cavity of NOG mice (data not shown). Recently, it has been reported that mouse $CD5^+$ B1 cells are deficient in both peritoneal and pleural cavities but not different in the spleen of chemokine $CXCL13^{-/-}$ mice [26]. Mouse chemokines may not function for human $CD5^+$ B1 cell homing and accumulation to the peritoneal cavity.

$CD5^+$ B1 cells are responsible for the production of IgM against various antigens and are known to play a role in the early response to bacterial and viral infections [27,28]. In our mouse, the serum levels of IgM correlated with the chimerism of human $CD45^+$ cells in the spleen (data not shown). Moreover, three models showed the increase of antigen-specific IgM but not IgG after immunization with DNP-KLH, regardless of the origin of $CD34^+$ cells (Fig. 6). Since the majority of mature B cells in the spleen expressed CD5, the antigen-specific IgM may be produced mainly by these $CD5^+$ B cells. The absence of accessory cells in purified $CD34^+$ cells might affect the differentiation of $CD5^-$ B2 cells. In fact, as we reported previously, when accessory cells were cotransplanted with ex vivo–expanded $CD34^+$ cells, IgGs were detected in the mice, albeit in a very small amount [9].

Human B-1 cells are mainly characterized to express CD5 and to localize in peritoneal cavities. In the present study, human B cells developed in NOG mice predominantly expressed CD5, but these $CD5^+$ B cells were found mainly in spleen and PB. In addition, these $CD5^+$B cells proliferated by phorbol 12-myristate 13-acetate (PMA) stimulation but not by IgM cross-linking (data not shown). According to Rothstein and Kolber [29], B1 cells possess such responding characters. Collectively, human $CD5^+$ B cells in NOG may possess B-1 cell characters but cannot migrate appropriately or cannot stay in peritoneal cavities due to the xenogeneic environment.

In summary we have demonstrated that hCB, hBM, and hMPB $CD34^+$ cells all possess a differentiation potential to be mature $CD5^+$ B cells in the spleen of NOG mice. Since few $CD5^-$ mature B cells were detectable in lymphoid tissues including BM and spleen, normal B2 development may require species-specific factors.

Acknowledgments

This study was supported by The Japan Society for the Promotion of Science (JSPS) grant no. JSPS-RFTF97100201; a Grant-In-Aid for Scientific Research and a Research Grant of The Science Frontier Program from the Ministry of Education, Science, Sports and Culture of Japan; Grant-In-Aid from the Ministry of Health and Wealth; and grants form Tokai University of Medicine Research Aid.

We thank Ken Sato and Fumihiko Kimura for helpful comments. We are also extremely grateful to Shinichi Kobayashi, Hiroki Torikai, Tetsuo Yamamoto, and Takuya Yamashita for sample collection. We thank for Animal Care Co. LTD for the excellent technique of animal breeding.

References

1. Ueda T, Tsuji K, Yoshino H, et al. Expansion of human NOD/SCID-repopulating cells by stem cell factor, Flk2/Flt3 ligand, thrombopoietin, IL-6, and soluble IL-6 receptor. J Clin Invest. 2000;105:1013–1021.
2. Wilpshaar J, Noort WA, Kanhai HH, Willemze R, Falkenburg JH. Engraftment potential into NOD/SCID mice of CD34$^+$ cells derived from human fetal liver as compared to fetal bone marrow. Haematologica. 2001;86:1021–1028.
3. Noort WA, Wilpshaar J, Hertogh CD, et al. Similar myeloid recovery despite superior overall engraftment in NOD/SCID mice after transplantation of human CD34$^+$ cells from umbilical cord blood as compared to adult sources. Bone Marrow Transplant. 2001;28:163–171.
4. Robin C, Pflumio F, Vainchenker W, Coulombel L. Identification of lymphomyeloid primitive progenitor cells in fresh human cord blood and in the marrow of nonobese diabetic–severe combined immunodeficient (NOD-SCID) mice transplanted with human CD34$^+$ cord blood cells. J Exp Med. 1999;189:1601–1610.
5. Pflumio F, Izac B, Katz A, Shultz LD, Vainchenker W, Coulombel L. Phenotype and function of human hematopoietic cells engrafting immune-deficient CB17-severe combined immunodeficiency mice and nonobese diabetic–severe combined immunodeficiency mice after transplantation of human cord blood mononuclear cells. Blood. 1996;88:3731–3740.
6. Larochelle A, Vormoor J, Hanenberg H, et al. Identification of primitive human hematopoietic cells capable of repopulating NOD/SCID mouse bone marrow: implications for gene therapy. Nat Med. 1996;2: 1329–1337.
7. Hogan CJ, Shpall EJ, McNulty O, et al. Engraftment and development of human CD34$^+$-enriched cells from umbilical cord blood in NOD/LtSz-scid/scid mice. Blood. 1997;90:85–96.
8. van der Loo JC, Hanenberg H, Cooper RJ, Luo FY, Lazaridis EN, Williams DA. Nonobese diabetic/severe combined immunodeficiency (NOD/SCID) mouse as a model system to study the engraftment and mobilization of human peripheral blood stem cells. Blood. 1998;92: 2556–2570.
9. Li C, Ando K, Kametani Y, et al. Reconstitution of functional human B lymphocytes in NOD/SCID mice engrafted with ex vivo expanded CD34$^+$ cord blood cells. Exp Hematol. 2002;30:1036–1043.
10. Hayakawa K, Hardy RR. Development and function of B-1 cells. Curr Opin Immunol. 2000;12:346–353.
11. Kantor AB, Herzenberg LA. Origin of murine B cell lineages. Annu Rev Immunol. 1993;11:501–538.
12. Nisitani S, Murakami M, Akamizu T, et al. Preferential localization of human CD5$^+$ B cells in the peritoneal cavity. Scand J Immunol. 1997;46:541–545.
13. Kantor AB, Merrill CE, Herzenberg LA, Hillson JL. An unbiased analysis of V(H)-D-J(H) sequences from B-1a, B-1b, and conventional B cells. J Immunol. 1997;158:1175–1186.
14. Klpps TJ. The CD5 B cell. Adv Immunol. 1989;47:117–185.
15. Kantor AB, Stall AM, Adams S, Herzenberg LA. Differential development of progenitor activity for three B-cell lineages. Proc Natl Acad Sci U S A. 1992;89:3320–3324.
16. Bhat NM, Kantor AB, Bieber MM, Stall AM, Herzenberg LA, Teng NN. The ontogeny and functional characteristics of human B-1 (CD5$^+$B) cells. Int Immunol. 1992;4:243–252.
17. Moretta A, Maccario R, Fagioli F, et al. Analysis of immune reconstitution in children undergoing cord blood transplantation. Exp Hematol. 2001;29:371–379.
18. Novelli EM, Ramirez M, Leung W, Civin CI. Human hematopoietic stem/progenitor cells generate CD5$^+$ B lymphoid cells in NOD/SCID mice. Stem Cells. 1999;17:242–252.
19. Ito M, Hiramatsu H, Kobayashi K, et al. NOD/SCID/γ(c)(null) mouse: an excellent recipient mouse model for engraftment of human cells. Blood. 2002;100:3175–3182.
20. Saito Y, Kametani Y, Hozumi K, et al. The in vivo development of human T cells from CD34$^+$ cells in the murine thymic environment. Int Immunol. 2002;14:1113–1124.
21. Yahata T, Ando K, Nakamura Y, et al. Functional human T lymphocyte development from cord blood CD34$^+$ cells in nonobese diabetic/Shi-scid, IL-2 receptor γ null mice. J Immunol. 2002;169:204–209.
22. Wardemann H, Boehm T, Dear N, Carsetti R. B-1a B cells that link the innate and adaptive immune responses are lacking in the absence of the spleen. J Exp Med. 2002;195:771–780.
23. Ikawa M, Kominami K, Yoshimura Y, Tanaka K, Nishimune Y, Okabe M. A rapid and non-invasive selection of transgenic embryos before implantation using green fluorescent protein (GFP). FEBS Lett. 1995;375:125–128.
24. Carvalho TL, Mota-Santos T, Cumano A, Demengeot J, Vieira P. Arrested B lymphopoiesis and persistence of activated B cells in adult interleukin 7$^{-/-}$ mice. J Exp Med. 2001;194:1141–1150.
25. Schiemann B, Gommerman JL, Vora K, et al. An essential role for BAFF in the normal development of B cells through a BCMA-independent pathway. Science. 2001;293:2111–2114.
26. Ansel KM, Harris RB, Cyster JG. CXCL13 is required for B1 cell homing, natural antibody production, and body cavity immunity. Immunity. 2002;16:67–76.
27. Bhat NM, Kantor AB, Bieber MM, Stall AM, Herzenberg LA, Teng NN. The ontogeny and functional characteristics of human B-1 (CD5$^+$B) cells. Int Immunol. 1992;4:243–252.
28. Schettino EW, Chai SK, Kasaian MT, Schroeder HW, Casali P. VHDJH gene sequences and antigen reactivity of monoclonal antibodies produced by human B-1 cells: evidence for somatic selection. J Immunol. 1997;158:2477–2489.
29. Rothstein TL, Kolber DL. Peritoneal B cells respond to phorbol esters in the absence of co-mitogen. J Immunol. 1988;140:2880–2885.

ELSEVIER

EXPERIMENTAL HEMATOLOGY

Experimental Hematology 31 (2003) 1323–1330

In vivo and in vitro differentiation of myocytes from human bone marrow–derived multipotent progenitor cells

Yukari Muguruma[a], Morayma Reyes[e], Yoshihiko Nakamura[a], Tadayuki Sato[a], Hideyuki Matsuzawa[a], Hiroko Miyatake[a], Akira Akatsuka[b], Johbu Itoh[b], Takashi Yahata[a,c], Kiyoshi Ando[a,c], Shunichi Kato[d], and Tomomitsu Hotta[a,c]

[a]*Division of Hematopoiesis, Research Center for Regenerative Medicine,* [b]*Teaching and Research Support Center,* [c]*Department of Hematology, and* [d]*Department of Cell Transplantation and Regenerative Medicine, Tokai University School of Medicine, Isehara, Kanagawa, Japan;* [e]*Stem Cell Institute, University of Minnesota Medical School, Minneapolis, Minn., USA*

(Received 19 June 2003; revised 26 August 2003; accepted 2 September 2003)

Objective. **Recent studies have shown that bone marrow (BM) contains cells capable of differentiating into myocytes in vivo. However, addition of demethylation drugs has been necessary to induce myocyte differentiation from BM cells in vitro, and precise mechanisms of BM cells' conversion to myocytes and the origin of those cells have not been established. We investigated the expression of myogenic markers during differentiation and maturation of myocytes from BM-derived multipotent adult progenitor cells (MAPC) under physiological culture condition.**

Materials and Methods. **Frozen BM samples from 21 healthy donors were used as a source of MAPC. To induce myocyte differentiation MAPC was cultured in the presence of 5% FCS, VEGF, bFGF, and IGF-1, and the expressions of myocyte markers were examined at various time points. We also investigated engraftment and differentiation of MAPC-derived myocytes in vivo.**

Results. **Frozen BM-derived MAPC, cultured under the physiological myogenic condition, demonstrated spatial expression patterns of several myocyte markers similar to that of authentic myocyte differentiation. When injected into murine muscles, MAPC treated with the myogenic condition engrafted and differentiated into myocyte marker–positive cells and myotubes in vivo.**

Conclusion. **For the first time, we were able to induce myocyte formation from BM cells under the physiological condition in vitro and demonstrated that treating cells with this condition prior to intramuscular injection increased efficiency of engraftment and differentiation in vivo.**

In the process of new muscle fiber formation, quiescent muscle precursor cells become activated, proliferate, differentiate, and fuse together to form multinucleated myotubes. Skeletal muscle satellite cells, residing between the basal lamina and plasma membrane of skeletal muscle fibers, have long been thought the only cell type responsible for postnatal muscle regeneration [1,2]. However, recently several reports have shown that other cells are also capable of differentiating into muscle fibers [3–5]. Among these are side population (SP) cells that are defined by their ability to efflux Hoechst 33342 dye and their distinctly small size [5], and skeletal muscle–derived $CD34^+/CD45^-$ (Sk-34) cells that are isolated from interstitial spaces of skeletal muscle based on their surface phenotype [4]. In addition to those endogenous myogenic cells, cells from other tissues, such as bone marrow (BM), demonstrated contribution to muscle regeneration [6–8]. Yet, for myocyte formation from BM-derived cells in vitro, addition of 5-azacytizine [9–11], known to cause epigenetic changes, seems to be essential, which precludes their clinical applications.

In the past few years, our concept regarding adult stem cells has been challenged by accumulating reports suggesting that differentiation potentials of tissue-specific stem

Offprint requests to: Yoshihiko Nakamura, Ph.D., Division of Hematopoiesis, Research Center for Regenerative Medicine, Tokai University School of Medicine, Boseidai, Isehara, Kanagawa 259-1193, Japan; E-mail: kahiko@is.icc.u-tokai.ac.jp

0301-472X/03 $–see front matter.
doi: 10.1016/j.exphem.2003.09.003

cells are more versatile than had previously been thought [12–14]. A number of in vivo studies, using experimental animal models as well as in humans, documented that following a BM transplant, cells of BM origin, i.e., donor cells, contributed to a number of organs including heart [15–18], intestinal epithelium [19], liver [20–24], skeletal muscle [7,8], kidney [25], and brain [26–30]. In any cases, however, frequencies of cells detected in recipient organs are very low, and the cause of this change in cell fate and the origin of these cells remain to be determined.

Recently, cells of remarkable proliferation and differentiation potential have been isolated from BM, muscle, and brain [31–35]. The cells, termed multipotent adult progenitor cells (MAPC), can contribute to all three germ layers both in vivo and in vitro. MAPCs of human and rodent can be culture-expanded more than 30 and 100 population doublings (PD), respectively. Since MAPC can be selected from autologous BM and have no evidence of teratoma formation, they may be used for systemic and local cell therapies. In this report, we show successful isolation of MAPC from human frozen BM and differentiation of MAPC into mesodermal and endodermal cell lineages. In addition, cells are able to form multinucleated myotubes in vitro without using DNA demethylation drugs. Importantly, MAPC-derived cells engraft, differentiate into myogenic marker–positive cells, and then form mature myotubes when injected into murine muscles.

Methods

Cytokines and media composition

Epidermal growth factor (EGF) was from Sigma Chemical Co. (St Louis, MO, USA), and platelet-derived growth factor BB (PDGF-BB), insulin like growth factor-1 (IGF-1), basic fibroblast growth factor (bFGF), fibroblast growth factor 4 (FGF4), hepatocyte growth factor (HGF), and vascular endothelial growth factor (VEGF) were all from R&D Systems (Minneapolis, MN, USA). Transforming growth factor β3 (TGF-β3) was from Genzyme (Cambridge, MA, USA). MAPC was expanded in medium composed of the followings (MAPC media): 60% DMEM (Gibco BRL, Grand Island, NY, USA), 40% MCDB-201, 1X insulin/transferrin/selenium (ITS), 1X linoleic acid bovine serum albumin (LA-BSA), 10^{-8}M dexamethasone, 10^{-4}M ascorbic acid 2-phosphate (all from Sigma), 10 ng/mL EGF, 10 ng/mL PDGF-BB, and 2% fetal calf serum (FCS). MAPC was differentiated in the presence of specific cytokines and reagents in the MAPC media without FCS, EGF, and PDGF unless otherwise indicated.

MAPC culture

Frozen BM obtained from 21 healthy donors (ages 11 to 47 years) following informed consent was used as a source of MAPC according to the institutional guidelines of Tokai University School of Medicine. BM mononuclear cells (BMMNCs) obtained by Ficoll-Paque (Lymphoprep, 1.077 g/mL; Nycomed, Oslo, Norway) density gradient centrifugation were plated onto human fibronectin (FN)-coated (5 ng/mL, BD Biosciences, Bedford, MA, USA) culture vessels at 1×10^5/cm^2 in MAPC media. Emerging adherent cells were expanded while maintaining cell densities below 5×10^3/cm^2. After 2 to 3 weeks, cells were trypsinized, treated with CD45 and GlyA immunomagnetic beads, and applied to a MACS depletion column (Miltenyi Biotec, Sunnyvale, CA, USA). Eluted cells devoid of highly adherent and large cells as well as reminiscent hematopoietic cells were plated at 10 cells per well in FN-coated 96-well plates and expanded at densities between 0.5 and 3×10^3/cm^2.

Karyotyping

Dividing cells were treated with 0.01 μg/mL colcemid overnight followed by lysis with hypotonic KCL and fixation in methanol/acetic acid.

Adipocyte differentiation

2×10^4/cm^2 MAPCs at 20 population doublings (PD) were cultured in DMEM-high glucose supplemented with 5% horse serum, 10^{-6} M dexamethasone, 0.2 mM indomethacin, 0.01 mg/mL insulin, and 0.5 mM 3-isobutyl-1-methyl-xanthine (all from Sigma) as described previously [36].

Chondrocyte differentiation

2.5×10^5 MAPCs at 25 PD were cultured as a pellet in DMEM-high glucose-based serum-free media containing 10^{-7}M dexamethasone, 50 μg/mL ascorbic acid 2-phosphate, ITS+ culture supplement (Collaborative Biomedical Products, Bedford, MA, USA), and 10 ng/mL TGF-β3 [37]. At the end of culture, pellets were processed for cryosectioning. Eight-μm sections of the pellet were stained with a type II collagen antibody (5B2.5, 1:100, Quartett, Berlin, Germany).

Osteoblast differentiation

5×10^3/cm^2 MAPCs at 25 PD were cultured in MAPC media containing 10^{-7}M dexamethasone and 10^{-2}M β-glycerophosphate [36]. Osteoblastic phenotype was assessed by histochemical staining for alkaline phosphatase expression and calcium deposition as well as quantification of calcium production in the culture supernatant using Calcium-E test kit (Wako Chemical, Osaka, Japan).

Endothelial differentiation

1.5×10^4/cm^2 MAPCs at 25 PD were cultured in serum-free media containing 10 ng/mL VEGF for 2 weeks or more with medium exchanges twice a week. Uptake of DiI-Ac-LDL (10 ng/mL, Biomedical Technologies Inc., Stoughton, MA, USA) and surface expressions of the following endothelial marker were analyzed: phycoerythirin (PE)-conjugated CD34 (BD Biosciences) and KDR (Sigma); fluorescein isothiocyanate (FITC)-conjugated CD105 (BD Biosciences), Tie-2 (Nichirei, Tokyo, Japan), and Ulex (Biogenesis, Poole, England); CD144 (Immunotech, Marseille, France), H1P12 (Chemicon, Temecula, CA, USA), and von Willenbrand Factor (vWF) (DAKO Co., Carpinteria, CA, USA) followed by GAM-FITC (BD Biosciences). For staining with vWF, cells were permeabilized with 1% paraformaldehyde (PFA).

Hepatocyte differentiation

3×10^4/cm^2 MAPCs at 30 PD were plated on 1% Matrigel (BD Biosciences) and maintained in serum-free media in the presence of 10 ng/mL FGF4 and 20 ng/mL HGF for 2 weeks with medium exchanges every 4 days. Expressions of hepatocyte-specific genes, namely albumin, CK18, and HNF3β, were assessed by reverse transcriptase polymerase chain reaction (RT-PCR), and albumin production was determined by using the Human Albumin ELISA

Quantification kit (Bethyl Laboratories, Inc., Montgomery, TX, USA). Immunofluorescent staining for albumin (HSA11, 1:1500, Sigma) was performed as described below.

Muscle differentiation

0.5 to 1 × 10^4/cm^2 MAPCs at 25 to 30 PD were plated in MAPC media containing 5% FCS, 10 ng/mL bFGF, 10 ng/mL VEGF, and 10 ng/mL IGF-1, but not EGF. Cells were allowed to become confluent and cultured for 2 weeks with medium exchanges every 4 days. At day 14, cells were fixed with 4% PFA and stained for myogenic markers as described below. For the time course expression of myogenic markers, cells were fixed at various time points and immunostained.

Lentiviral transduction of MAPCs

0.3 × 10^3/cm^2 MAPCs at 20 PD were cultured in MAPC media in the presence of supernatant of lentivirus harboring enhanced green fluorescent protein (EGFP)-encoded gene at an multiplicity of infection (MOI) of 16 for 20 hours [38]. Efficiency of EGFP transduction was determined by flow cytometric analysis.

Immunostaining

Cultured cells were fixed with 4% PFA for 10 minutes at room temperature. For enzyme immunohistochemistry, endogenous peroxidase was quenched with 0.3% peroxidase in 70% methanol for 30 minutes. Nonspecific binding of antibodies was blocked by incubating cells with 5% serum from animals in which secondary antibodies were raised. For staining of cytoplasmic and nuclear proteins, 0.01% triton-X-100 was added. Cells were incubated overnight at 4°C with the following primary antibodies at the indicated concentrations: MyoD (5.8A, 1:20) and myogenin (F5D, 1:200) from DAKO; skeletal (SK) myosin (MY-32, 1:1600), α-actinin (EA-53, 1:800), and desmin (DE-U-10, 1:40) from Sigma. Specific binding of respective antibodies was visualized as the brown reaction product of peroxidase substrate 3, 3′-diaminobenzidine (DAB, Sigma) using ABC kit (Vector Laboratories, Inc., Burlingame, CA, USA) or as fluorescent signals.

Immunoelectron microscopy

MAPCs were cultured in Lab-Tek Permanox chamber slide (Nunc) as described above to induce muscle differentiation. After fixing with 4% PFA, cells were stained for SK-myosin and prepared for electron microscopic analysis as described previously [39].

RT-PCR

Total RNA was extracted from undifferentiated MAPCs and MAPCs induced to differentiate to hepatocytes. After cDNA synthesis, products were amplified using sequence-specific primers under the following condition: 94°C for 4 minutes//94°C for 30 seconds, 60°C for 30 seconds, 72°C for 1 minutes (35 cycles)// 72°C for 7 minutes. The following paired primers were used: albumin forward (F) 5′TGCTTGAATGTGCTGATGACAGGG-3′ and reverse (R) 5′-AAGGCAAGTCAGCAGGCATCTCATC-3′ (162 base pair [bp]); CK18 F 5′-CTCTGGATTGACTGTGGAAGT-3′ and R 5′-TGGTACTCTCCTCAATCTGCTG-3′ (149 bp); HNF3β F 5′-CGCAGATACCTCCTACTACCAG-3′ and R 5′-TGGCCT-TCTGTTTGGGACGGAA-3′ (257 bp).

Transplantation of MAPC into murine muscle

EGFP-transduced undifferentiated MAPCs or MAPCs treated with myogenic condition for 3 days (2 × 10^5) were suspended in 25 μL 1% carboxymethyl cellulose (Sigma) and injected into tibialis anterior (TA) muscles of irradiated (250 cGy) 6- to 8-week-old NOD/Shi-scid (NOD/SCID) mice (CLEA JAPAN, Tokyo, Japan). Twenty-four hours prior to transplantation, muscle regeneration was induced by injecting 25 μL of 10^{-5} M cardiotoxin (Sigma) into TA muscles. Nine and 27 weeks after cell injection, mice were perfused with warm phosphate-buffered saline (PBS) followed by 4% PFA. TA muscles were removed, immersed in 4% PFA overnight at 4°C, treated with graded sucrose/PBS (5–25%), and then quick-frozen in isopentane. Seven-μm sections were first examined for the presence of EGFP-expressing cells, and the same sections were stained for EGFP (1:500, MBL, Nagoya, Japan) or myogenic markers, α-actinin, and SK-myosin.

PCR Southern blot

Genomic DNA was extracted from a single cryosection of TA muscles from each animal by standard extraction protocols. One-tenth of DNA samples were amplified to detect a 558-bp fragment of EGFP gene using the RNA PCR kit (Takara) under the following conditions: 94°C for 1 minute//94°C for 1 minute, 68°C for 1 minute, 72°C for 1 minute (35 cycles)//72°C for 7 minutes. PCR products were separated on 3.0% agarose gel, transferred to nylon membranes, and hybridized with a biotin-labeled random-primed EGFP probe. Primers for EGFP were F 5′-CAAGTT-CAGCGTGTCCGGCG-3′ and R 5′-GGGGTCTTTGCTCAG-GGCGG-3′.

Results

Culture of MAPC from frozen bone marrow samples

Although purification of MAPC using fresh BM and other tissues was well described in recently published papers, isolation of MAPC from frozen samples has not been done. We sought to use stock frozen BM samples as a source of MAPC, taking advantage of their readiness. First we followed the protocol for MAPC isolation from fresh human BM. Briefly, thawed BMMNCs were subjected to density gradient centrifugation to eliminate dead cells and cell debris. Centrifuged cells (3.8–13.8% of original BMMNCs) were negatively selected by the expression of CD45 and GlyA using a MACS depletion column. Purity (1–20%) and recovery (0.1–0.5% of centrifuged cell) of $CD45^-$ $GlyA^-$ cells were not satisfactory, probably owing to a high tendency of thawed cells to aggregate within a column. Addition of 5 U/mL DNase to washing medium and elution buffer did not improve purity (13.8%) of recovered cells. We therefore plated cells without MACS depletion. Clonal growth of adherent cells was observed after 4 to 7 days, and those cells were propagated for 2 to 3 weeks with care to keep cell densities below 5 × 10^3 cells/cm^2. Cells were then applied to the MACS column, plated at 10 cells/well in 96 plates, and expanded by passaging every 2 to 3 days. Cell doubling time was 48 to 60 hours (Fig. 1A). MAPC usually appeared as polygonal-shaped cells with scant cytoplasm and had granules around nuclei (Fig. 1B). We detected no karyotype abnormalities (Fig. 1C). Of the 21 frozen samples used in the experiment, we succeeded in

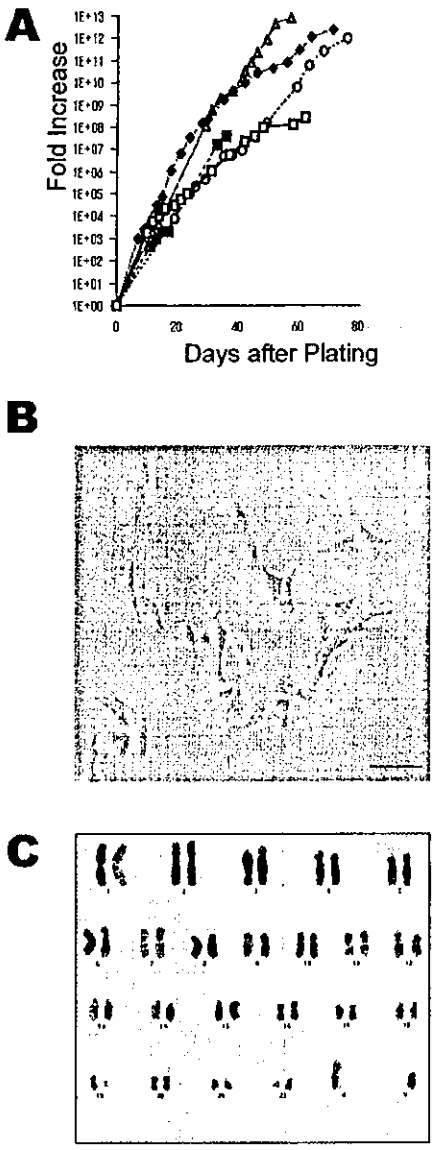

Figure 1. Characteristics of human frozen BM-derived MAPC. Human frozen BM-derived cells were maintained at cell densities between 0.5 and 3×10^3 cells/cm^2 and were enumerated using a hemocytometer at each passage. Shown are growth curves of representative MAPCs derived from 5 different donors (**A**). Typical morphology of MAPC (**B**, bar: 50 μm). A representative result of cytogenetic analysis at 30 PD (**C**).

expanding beyond 20, 30, and 40 PD for 13, 5, and 3 donors, respectively.

MAPC differentiation into adipocytes, chondrocytes, osteoblasts, endothelial cells, and hepatocytes

We then examined whether cells isolated in our method have the ability to differentiate into multiple cell lineages. Cells were cultured under conditions specific to the respective lineages as described in Materials and methods. Cells turned into adipocytes in as early as 8 days under the adipogenic condition (Fig 2A). Cells cultured in the presence of TGF-β3 as a pellet expressed type II collagen (Fig. 2B), a chondrocyte-specific protein. Cells cultured in the presence of high concentration of dexamethasone and β-glycerophosphate exhibited the phenotype and function of osteoblasts, namely alkaline phosphatase expression and calcium production, respectively (Fig. 2C). Average calcium production at day 21 was 105.7 ±16.4 μg/well (2×10^4 inoculated cells, n = 5). Cells cultured in serum-free media supplemented

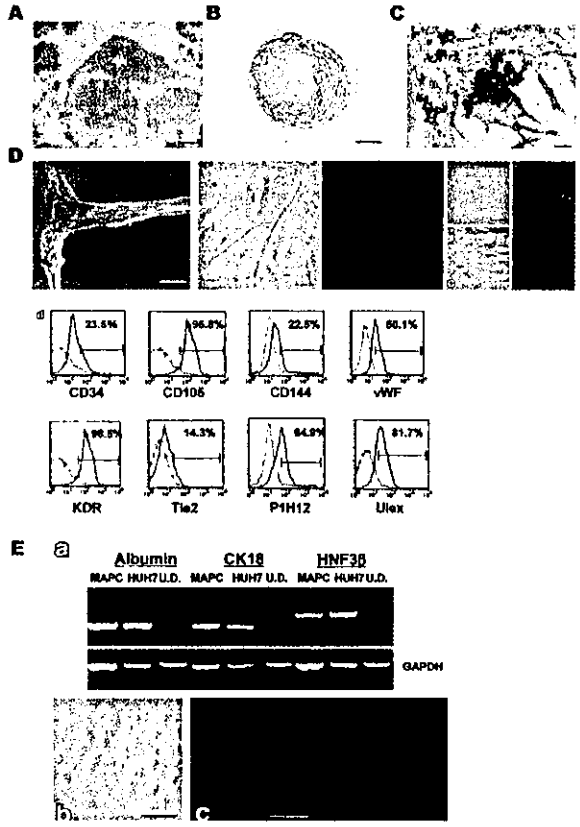

Figure 2. Multilineage differentiation of human frozen BM-derived MAPC. Cells were cultured under differentiation conditions specific for adipocyte, chondrocyte, osteoblast, endothelial cell, and hepatocyte as described. Differentiation into respective lineages was identified using histochemical staining, immunohistochemical staining, flow cytometry, and RT-PCR methods. Oil red O staining revealed the presence of numerous oil droplets in the cytoplasm (**A**, bar: 25 μm). Cryosections of cell pellets were stained positive for chondrocyte-specific type II collagen (**B**, bar: 100 μm). Cells demonstrated alkaline phosphatase expression, and the presence of $CaPO_4$ crystals was visualized using von Kossa staining method (**C**, bar: 50 μm). Cells formed tube-like structure (**D,a**) and incorporated DiI-Ac-LDL (**D,b**). HUVEC, human endothelial cells, and OP9, a mouse BM stromal cell line, were used as positive and negative controls, respectively, for DiI-Ac-LDL incorporation (**D,c**, bars; a: 100 μm, b and c: 25 μm). A number of endothelial markers were detected by flow cytometric analysis (**D,d**). Hepatocyte-specific gene expression was detected by RT-PCR (**E,a**). U.D.: Undifferentiated MAPC. HUH7 human hepatic cancer cells were used as positive controls. Bright-field and immunostaining for albumin photos of differentiated cells are shown (**E,b&c**, bars: 25 μm). Isotype control (**E,c** right photo).

with VEGF for 3 weeks formed tube-like structures and incorporated DiI-Ac-LDL (Fig. 2D, a and b). A number of cell surface (CD34, CD105, CD144, KDR, Tie-2, Ulex, H1P12) and intracellular proteins (vWF) specific to mature endothelial cells were detected by flow cytometric analysis (Fig. 2D, d). Differentiation into hepatocyte lineage required that cells were fully confluent before undergoing differentiation conditions; otherwise cells detached from culture wells and died within first 7 days. After 14 days, cells expressed genes for albumin, CK18, and HNF3β and showed morphological resemblance to cultured hepatocytes (Fig. 2E, a and b). Albumin protein expression was visualized by immunofluorescent staining (Fig. 2E, c). Production of human albumin was detected in the culture supernatant at day 14 (1.99 ± 1.16 ng/mL, 3×10^4 inoculated cells, n = 6). The results demonstrated that MAPC established in our condition can differentiate into mesodermal and endodermal lineages as described previously [33–35].

MAPC differentiation into striated myotubes in vitro

Having established MAPC capable of differentiating into mesodermal and endodermal cell lineages from frozen BM samples, we decided to investigate myogenic ability of MAPC. Although a previous report has shown that MAPC can be induced to express several myocyte markers when treated with 5-azacytizine [33], we tested whether myotubes can be formed in more physiological conditions. MAPCs were plated at 0.5 to $1 \times 10^4/cm^2$ in MAPC medium containing 5% FCS, VEGF, bFGF, IGF-1 without EGF and allowed to become confluent. Around day 10, multinucleated tube formation was noted (Fig. 3A, a). Those tubes stained positive for α-actinin and SK-myosin (Fig. 3A, c and d) and demonstrated the presence of striated myofibers in the cytoplasm (Fig. 3A, b). A time course study was conducted to examine the expression of muscle-specific markers (Fig. 3B). By day 4, the presence of mononuclear cells expressing MyoD was apparent, and the frequency peaked at day7 (28–40%), then declined thereafter. There followed increases in the number of myogenin-, α-actinin-, and SK-myosin-expressing mononuclear cells and multinucleated tubes. Proportions of multinucleated myotubes positive for above-mentioned markers varied among the fields examined (10–42%). It appeared that in situ proliferation of mononuclear cells positive for MyoD and subsequent fusion of those cells formed multinucleated myotubes.

Transplantation of MAPC into murine muscles

In order to investigate whether MAPC can engraft and differentiate into mature muscles in vivo, we injected undifferentiated MAPCs or MAPCs treated with the myogenic condition into regenerating murine TA muscles. First, we transduced EGFP gene into MAPCs (Fig. 4A). Transduced cells were able to form multinucleated tubes that stained positive for desmin, α-actinin, and SK-myosin in vitro (Fig. 4B, a–c). When undifferentiated MAPCs were injected, few EGFP-transduced cells were observed in histological sections of 3

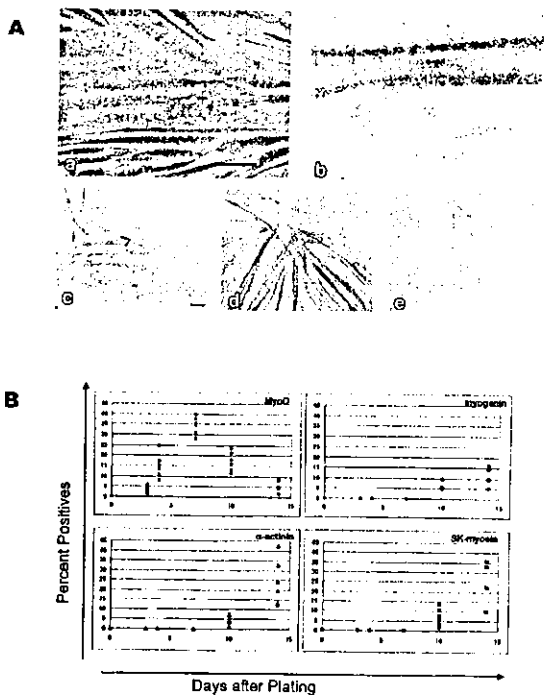

Figure 3. Myogenic differentiation of MAPC in vitro. Cells cultured in the presence of 5% FCS, VEGF, bFGF, IGF-1 fused and formed multinucleated tubes (**A,a**, bar: 100 μm). An immunoelectron microscopic photograph showing prominent striated myofibers in the cytoplasm (**A,b**, original magnification: ×11,000). The tubes were stained positive for α-actinin and SK-myosin (**A,c&d**, bars: 100 μm). Isotype control (**A,e**). For the time course analysis, cells were cultured in the 4-well chamber slides under the myogenic condition, fixed at the indicated time points, and stained for MyoD, myogenin, α-actinin, and SK-myosin. Six random fields (78 to 419 cells/field) were examined under the microscope, and cells were enumerated with assistance of Zeiss KS400. For MyoD and myogenin expressions, percent of marker-positive nuclei is shown. For α-actinin and SK-myosin expressions, percent of nuclei in the respective marker-positive cytoplasm is shown (**B**).

out of 4 animals. Results of Southern blot analysis were consistent with histological observation (Fig. 5A, animals 1–4). However, these EGFP-positive cells were confined in the scar tissue area and did not express myocyte marker (Fig. 5B, a and b). In contrast, 9 weeks after intramuscular injection of MAPCs treated with myogenic condition, numerous EGFP-positive mononuclear cells were seen in the periphery of regenerating muscles (Fig. 5B, d and f). The presence of EGFP gene was confirmed by Southern blot analysis (Fig. 5A, animals 5 and 6). Importantly, EGFP-expressing human cells stained positive for α-actinin and SK-myosin (Fig. 5B, c and e). Furthermore, in animals sacrificed at 27 weeks these EGFP-expressing mononuclear cells fused together and formed myotubes, in which prominent alignment of α-actinin and SK-myosin was clearly visualized by immunofluorescent staining (Fig. 5C). The result indicated that human MAPC can engraft and differentiate into mature myotubes in vivo. Moreover, the efficiency of engraftment is greatly

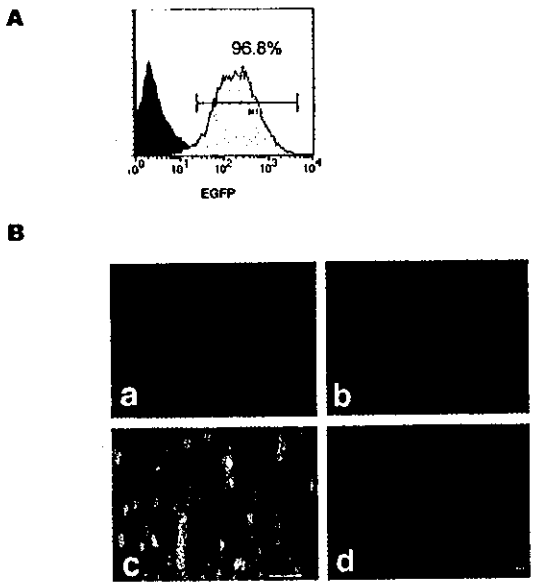

Figure 4. Lentiviral transduction of MAPC and differentiation into myocyte in vitro. Cells were transduced with a lentivirus vector. The transduction efficiency was assessed by the expression of EGFP protein using FACS (**A**). Transduced cells were cultured under the myogenic condition for 14 days and stained for myocyte markers, desmin (**B,a**), α-actinin (**B,b**), and SK-myosin (**B,c**). Isotype control (**B,d**). Bars; a, b, c: 50 μm, d: 50 μm.

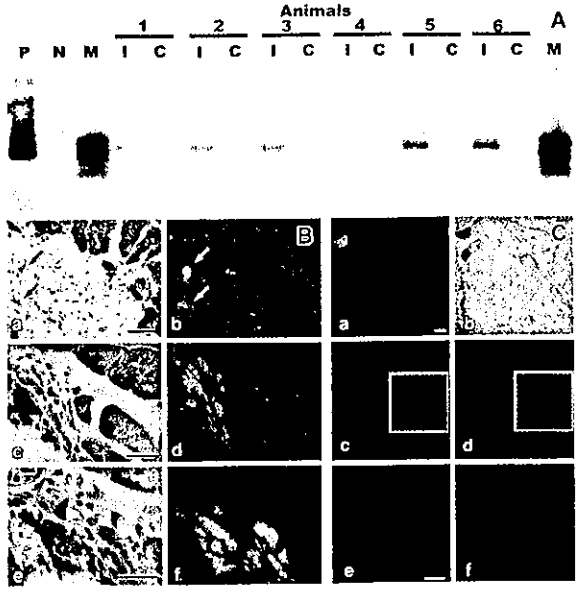

Figure 5. Engraftment of MAPC-derived myocyte in murine muscle. Undifferentiated MAPCs (animals 1–4) or MAPCs treated with myogenic condition for 3 days (animals 5 and 6) were injected into TA muscle of NOD/SCID mice. Nine weeks after transplantation, the presence of EGFP-transduced cells was detected by PCR–Southern blot analysis (**A**) and immunohistochemistry (**B**). P: sample positive, i.e., muscle of GFP mouse; N: sample negative, i.e., muscle of noninjected NOD/SCID mouse; M: molecular weight markers; I: injected muscle; C: contralateral muscle. Scattered EGFP-expressing cells were seen within the scar tissue in the muscle of undifferentiated MAPC-injected animals (**B,b**, arrows, animal 1). These cells did not stain with SK-myosin (**B,a**, arrows). Note the presence of EGFP-expressing cells stained positive for α-actinin (**B,c**) and SK-myosin (**B,e**) in differentiated MAPC-injected TA muscle (animal 5). Cryosections from TA muscle of differentiated MAPC-injected animals at 27 weeks were examined (**C**). Dark-filed observation revealed the presence of EGFP-expressing mature myotubes (**C,a**). An adjacent section of (a) was immunostained using a GFP antibody (**C,b**). Immunofluorescent staining for α-actinin (**C,c**) and SK-myosin (**C,d**). High magnification of the insets in c (**C,e**) and d (**C,f**) are merged with EGFP photos. The alignment of α-actinin and SK-myosin within EGFP-expressing myotubes is seen. Bars in **B** and **C** represent 25 μm.

enhanced by pretreating MAPC with clinically applicable myogenic condition.

Discussion

We report that MAPC can be isolated from human frozen BM samples and culture-expanded beyond 40 PD. In agreement with previous reports, isolated cells are able to differentiate into multiple cell lineages. In addition, multinucleated myotubes can be derived from cells established in our condition in the absence of DNA demethylation drugs in vitro, and MAPC-derived myocytes engraft in murine muscles.

Over the past 5 years, there has been overwhelming evidence to suggest plasticity of once thought "tissue-specific" stem cells. Most studies, however, have established donor cell contribution solely by in vivo experiment, and the frequency of the donor cells is usually very low. Many, if not all, studies are still waiting for independent confirmation. To understand how cells differentiate into lineages other than where they reside and the underlying mechanisms of cell fate changes, reliable in vitro models are essential. Recently, Reyes and colleagues reported isolation of MAPC that is capable of differentiating into mesodermal, endodermal, and ectodermal lineages both in vivo and in vitro [31–35,40]. Identification of MAPC attracted substantial excitement; however, at the same time it called some skepticism owing to the difficulties of isolating and maintaining MAPC. Here we demonstrated MAPC isolation from stock frozen human BM samples. Using a similar technique previously described for isolation of MAPC from rodent fresh BM, we established MAPC from 21 samples by expanding 20 to over 40 PD in vitro. Age of donors and conditions for freezing and/or storage of samples may account for reasons of such variation in cells' ability to proliferate in vitro. Those expanded cells differentiated into adipocytes, chondrocytes, osteoblasts, endothelial cells, and hepatocytes. In all, MAPC can be isolated not only from fresh but also from frozen BM and be differentiated into mesodermal and endodermal lineages.

Skeletal muscle regeneration occurs in repair of injured muscles. Recently, investigators found cells other than satellite cells could contribute to growth and maintenance of

postnatal skeletal muscle. For instance, following intramuscular transplantation of muscle-derived $CD45^-$ SP cells, regenerating muscle fibers exhibiting donor cell marker were detected, and SP cells were able to form myogenic colonies in methylcellulose cultures in vitro [5]. However, other reports failed to detect in vitro myocyte differentiation ability of SP cells [41]. Another type of muscle-derived myogenic cells, Sk-34, were also able to differentiate into skeletal muscle in vivo and in vitro [4]. Although these muscle-derived myogenic cells are promising candidates to replace injured muscle in cell therapy, surgical operations are necessary to collect donor cells [42]. Since muscle-derived myogenic cells are not expandable, obtaining sufficient number of cells is severely invasive to donors. Aside from the endogenous myogenic cell sources, BM contains cells capable of contributing to skeletal muscle regeneration [6–8]. Marrow cells are far more accessible compared to muscle-derived cells that require surgery, and can be culture-expanded. Use of marrow cells in potential therapy excited considerable interest. The conversion of marrow cells to muscle cells is, however, a rare event, and prestimulation of marrow cells into muscle lineages in vitro could augment the marrow cell contribution in muscle regeneration in vivo. While muscle-derived cells can be matured in the presence of cytokines and FCS [4,43], it appears that addition of demethylation drugs in culture system [9–11] or transduction of MyoD into cells [44] is essential to induce muscle formation from marrow cells in vitro, which is rather artificial and may not be ideal for clinical applications.

In this study, we demonstrated myocyte formation from human frozen BM-derived MAPC both in vitro and in vivo. We were able to induce myocyte formation in the presence of well-characterized cytokines VEGF, bFGF, and IGF-1 in vitro. While we did not conduct comparative studies for myogenic conditions, 5% FCS is preferable to 2% FCS, and the presence of EGF negatively affects myocyte formation by stimulating proliferation of cells other than myocyte lineage. In our culture system, MyoD-expressing mononuclear cells were evident as early as 3 days after stimulation. The frequency of cells positive for MyoD increased until day 7 and declined, which was followed by the appearance of myogenin-, α-actinin-, and SK-myosin-expressing cells and myotubes. This expression pattern resembles authentic muscle differentiation [43], suggesting that our culture system mimics physiological environment of muscle differentiation. The cytokines we used in this study may play roles in muscle differentiation and regeneration after injury as IGF-1 is implicated for proliferation and differentiation of myoblast [2]. By day 14 of culture, cells formed multinucleated myotubes. The proportion of muscle marker–positive cells accounted as much as 42% in the counted fields. Such a high efficiency of muscle cell generation in vitro has never been described. Based on this, MAPC, in conjunction with our physiological culture method, could well be considered as alternative cell source for muscle replacement therapy. Furthermore, cells generated in our culture system demonstrated engraftment and differentiation into muscle marker–positive cells and mature myotubes in murine muscles, the first demonstration of human BM-derived cell engraftment in skeletal muscle of xenogeneic mouse host. As we hypothesized, treating cells with myogenic condition prior to intramuscular injection appeared effective in augmenting human MAPC engraftment in murine host. Although the levels of engraftment were not much different between myogenic treated and nontreated groups as determined by Southern blot analysis, clusters of EGFP and myogenic marker–expressing cells were obvious only in histological sections of animals injected with pretreated cells. In addition to the environmental cue from the host animal, driving signals may be necessary for conversion of untreated human MAPC into myocytes in xenogeneic murine host. Twenty-seven weeks after intramuscular injection of pretreated MAPC, the presence of EGFP-expressing myotubes was unmistakable. They exhibited bona fide muscle morphology and the alignment of α-actinin and SK-myosin. This indicates that fusion of EGFP-expressing mononuclear cells occurred during the two time points we analyzed. We are now investigating chronological events during muscle regeneration after intramuscular injection of MAPC.

At this point developmental origin of MAPC remains elusive, as do the relationships between myogenic MAPC and muscle-derived myogenic cells. It has been quite difficult to assess biological mechanisms of myocyte differentiation from BM-derived cells because of the lack of appropriate culture system. Here we showed for the first time the resemblances of BM-derived and endogenous myogenic cells; they differentiated and matured in the presence of cytokines and FCS, and they followed similar spatial gene expressions in vitro. A question remains whether MAPC contains subpopulations and/or progenitors of endogenous myogenic cells, such as satellite cells, SP cells, and Sk-34, or if MAPC is a distinct population. Further studies are required to answer this important question. In summary, we have shown that MAPC isolated from frozen human BM can be differentiated into muscle marker–positive cells in clinically applicable culture condition and those cells can engraft and form multinucleated myotubes in murine skeletal muscles. Our findings could be used to study the mechanisms of muscle cell conversion from marrow cells and will be helpful for development of cell therapy using BM cells.

Acknowledgments

We thank Dr. Catherine Verfaillie for her valuable advice, Tamaki Saso and Tomoko Nakai for their excellent technical assistance, Drs. Tetsuro Tamaki and Hiroshi Kawada for helpful discussions, and all members of Research Center for Regenerative Medicine and Dr. Charles Peters for their support. This work is supported by a grant-in-aid for a Research Grant of the Science Frontier Program from the Ministry of Education, Culture, Sports, Science and Technology of Japan.

References

1. Grounds MD. Towards understanding skeletal muscle regeneration. Pathol Res Pract. 1991;187:1–22.
2. Seale P, Rudnicki MA. A new look at the origin, function, and "stem-cell" status of muscle satellite cells. Dev Biol. 2000;218:115–124.
3. Lee JY, Qu-Petersen Z, Cao B, et al. Clonal isolation of muscle-derived cells capable of enhancing muscle regeneration and bone healing. J Cell Biol. 2000;150:1085–1100.
4. Tamaki T, Akatsuka A, Ando K, et al. Identification of myogenic-endothelial progenitor cells in the interstitial spaces of skeletal muscle. J Cell Biol. 2002;157:571–577.
5. McKinney-Freeman SL, Jackson KA, Camargo FD, Ferrari G, Mavilio F, Goodell MA. Muscle-derived hematopoietic stem cells are hematopoietic in origin. Proc Natl Acad Sci U S A. 2002;99:1341–1346.
6. Gussoni E, Soneoka Y, Strickland CD, et al. Dystrophin expression in the mdx mouse restored by stem cell transplantation. Nature. 1999; 401:390–394.
7. Ferrari G, Cusella-De Angelis G, Coletta M, et al. Muscle regeneration by bone marrow-derived myogenic progenitors. Science. 1998;279: 1528–1530.
8. LaBarge MA, Blau HM. Biological progression from adult bone marrow to mononucleate muscle stem cell to multinucleate muscle fiber in response to injury. Cell. 2002;111:589–601.
9. Makino S, Fukuda K, Miyoshi S, et al. Cardiomyocytes can be generated from marrow stromal cells in vitro. J Clin Invest. 1999;103:697–705.
10. Wakitani S, Saito T, Caplan AI. Myogenic cells derived from rat bone marrow mesenchymal stem cells exposed to 5-azacytidine. Muscle Nerve. 1995;18:1417–1426.
11. Tomita S, Li RK, Weisel RD, et al. Autologous transplantation of bone marrow cells improves damaged heart function. Circulation. 1999; 100:II247–256.
12. Bjornson CR, Rietze RL, Reynolds BA, Magli MC, Vescovi AL. Turning brain into blood: a hematopoietic fate adopted by adult neural stem cells in vivo. Science. 1999;283:534–537.
13. Clarke DL, Johansson CB, Wilbertz J, et al. Generalized potential of adult neural stem cells. Science. 2000;288:1660–1663.
14. Galli R, Borello U, Gritti A, et al. Skeletal myogenic potential of human and mouse neural stem cells. Nat Neurosci. 2000;3:986–991.
15. Jackson KA, Majka SM, Wang H, et al. Regeneration of ischemic cardiac muscle and vascular endothelium by adult stem cells. J Clin Invest. 2001;107:1395–1402.
16. Orlic D, Kajstura J, Chimenti S, et al. Bone marrow cells regenerate infarcted myocardium. Nature. 2001;410:701–705.
17. Shimizu K, Sugiyama S, Aikawa M, et al. Host bone-marrow cells are a source of donor intimal smooth-muscle-like cells in murine aortic transplant arteriopathy. Nat Med. 2001;7:738–741.
18. Sata M, Saiura A, Kunisato A, et al. Hematopoietic stem cells differentiate into vascular cells that participate in the pathogenesis of atherosclerosis. Nat Med. 2002;8:403–409.
19. Okamoto R, Yajima T, Yamazaki M, et al. Damaged epithelia regenerated by bone marrow–derived cells in the human gastrointestinal tract. Nat Med. 2002;8:1011–1017.
20. Alison MR, Poulsom R, Jeffery R, et al. Hepatocytes from non-hepatic adult stem cells. Nature. 2000;406:257.
21. Theise ND, Nimmakayalu M, Gardner R, et al. Liver from bone marrow in humans. Hepatology. 2000;32:11–16.
22. Theise ND, Badve S, Saxena R, et al. Derivation of hepatocytes from bone marrow cells in mice after radiation-induced myeloablation. Hepatology. 2000;31:235–240.
23. Petersen BE, Bowen WC, Patrene KD, et al. Bone marrow as a potential source of hepatic oval cells. Science. 1999;284:1168–1170.
24. Lagasse E, Connors H, Al-Dhalimy M, et al. Purified hematopoietic stem cells can differentiate into hepatocytes in vivo. Nat Med. 2000;6:1229–1234.
25. Masuya M, Drake CJ, Fleming PA, et al. Hematopoietic origin of glomerular mesangial cells. Blood. 2003;101:2215–2218.
26. Mezey E, Chandross KJ, Harta G, Maki RA, McKercher SR. Turning blood into brain: cells bearing neuronal antigens generated in vivo from bone marrow. Science. 2000;290:1779–1782.
27. Azizi SA, Stokes D, Augelli BJ, DiGirolamo C, Prockop DJ. Engraftment and migration of human bone marrow stromal cells implanted in the brains of albino rats--similarities to astrocyte grafts. Proc Natl Acad Sci U S A. 1998;95:3908–3913.
28. Brazelton TR, Rossi FM, Keshet GI, Blau HM. From marrow to brain: expression of neuronal phenotypes in adult mice. Science. 2000; 290:1775–1779.
29. Eglitis MA, Mezey E. Hematopoietic cells differentiate into both microglia and macroglia in the brains of adult mice. Proc Natl Acad Sci U S A. 1997;94:4080–4085.
30. Kopen GC, Prockop DJ, Phinney DG. Marrow stromal cells migrate throughout forebrain and cerebellum, and they differentiate into astrocytes after injection into neonatal mouse brains. Proc Natl Acad Sci U S A. 1999;96:10711–10716.
31. Jiang Y, Vaessen B, Lenvik T, Blackstad M, Reyes M, Verfaillie CM. Multipotent progenitor cells can be isolated from postnatal murine bone marrow, muscle, and brain. Exp Hematol. 2002;30:896–904.
32. Jiang Y, Jahagirdar BN, Reinhardt RL, et al. Pluripotency of mesenchymal stem cells derived from adult marrow. Nature. 2002;418:41–49.
33. Reyes M, Lund T, Lenvik T, Aguiar D, Koodie L, Verfaillie CM. Purification and ex vivo expansion of postnatal human marrow mesodermal progenitor cells. Blood. 2001;98:2615–2625.
34. Reyes M, Dudek A, Jahagirdar B, Koodie L, Marker PH, Verfaillie CM. Origin of endothelial progenitors in human postnatal bone marrow. J Clin Invest. 2002;109:337–346.
35. Schwartz RE, Reyes M, Koodie L, et al. Multipotent adult progenitor cells from bone marrow differentiate into functional hepatocyte-like cells. J Clin Invest. 2002;109:1291–1302.
36. Pittenger MF, Mackay AM, Beck SC, et al. Multilineage potential of adult human mesenchymal stem cells. Science. 1999;284:143–147.
37. Mackay AM, Beck SC, Murphy JM, Barry FP, Chichester CO, Pittenger MF. Chondrogenic differentiation of cultured human mesenchymal stem cells from marrow. Tissue Eng. 1998;4:415–428.
38. Oki M, Ando K, Hagihara M, et al. Efficient lentiviral transduction of human cord blood $CD34^+$ cells followed by their expansion and differentiation into dendritic cells. Exp Hematol. 2001;29:1210–1217.
39. Tamaki T, Akatsuka A, Yoshimura S, Roy RR, Edgerton VR. New fiber formation in the interstitial spaces of rat skeletal muscle during postnatal growth. J Histochem Cytochem. 2002;50:1097–1111.
40. Zhao LR, Duan WM, Reyes M, Keene CD, Verfaillie CM, Low WC. Human bone marrow stem cells exhibit neural phenotypes and ameliorate neurological deficits after grafting into the ischemic brain of rats. Exp Neurol. 2002;174:11–20.
41. Asakura A, Seale P, Girgis-Gabardo A, Rudnicki MA. Myogenic specification of side population cells in skeletal muscle. J Cell Biol. 2002;159:123–134.
42. Grounds MD, White JD, Rosenthal N, Bogoyevitch MA. The role of stem cells in skeletal and cardiac muscle repair. J Histochem Cytochem. 2002;50:589–610.
43. Seale P, Sabourin LA, Girgis-Gabardo A, Mansouri A, Gruss P, Rudnicki MA. Pax7 is required for the specification of myogenic satellite cells. Cell. 2000;102:777–786.
44. Toma C, Pittenger MF, Cahill KS, Byrne BJ, Kessler PD. Human mesenchymal stem cells differentiate to a cardiomyocyte phenotype in the adult murine heart. Circulation. 2002;105:93–98.

myocardial infiltration by tumor. A cardiac mass seen on echocardiography or magnetic resonance imaging suggests the diagnosis of cardiac lymphoma, and positive pericardial effusion cytology, endomyocardial biopsy, or direct biopsy via thoracotomy confirms the diagnosis.

Michael A. Thompson, Amy Harker-Murray, Adam J. Locketz, and Panithaya Chareonthaitawee
Mayo Clinic, Rochester, MN

Authors' Disclosures of Potential Conflicts of Interest

The authors indicated no potential conflicts of interest.

REFERENCES

1. Addis BJ, Isaacson PG: Large cell lymphoma of the mediastinum: A B-cell tumour of probable thymic origin. Histopathology 10:379-390, 1986
2. Lamarre L, Jacobson JO, Aisenberg AC, et al: Primary large cell lymphoma of the mediastinum: A histologic and immunophenotypic study of 29 cases. Am J Surg Pathol 13:730-739, 1989
3. Boring CC, Squires TS, Tong T, et al: Cancer statistics, 1994. CA Cancer J Clin 44:7-26, 1994
4. Lam KY, Dickens P, Chan AC: Tumors of the heart: A 20-year experience with a review of 12,485 consecutive autopsies. Arch Pathol Lab Med 117:1027-1031, 1993
5. Chim CS, Chan AC, Kwong YL, et al: Primary cardiac lymphoma. Am J Hematol 54:79-83, 1997
6. Chalabreysse L, Berger F, Loire R, et al: Primary cardiac lymphoma in immunocompetent patients: A report of three cases and review of the literature. Virchows Arch 441:456-461, 2002

DOI: 10.1200/JCO.2004.12.100

CASE 3. $CD8^+$ T-Cell Prolymphocytic Leukemia

A 33-year-old Japanese woman was referred because of leukocytosis with increased abnormal lymphocytes on a routine blood test. She was completely asymptomatic. Physical examination was essentially normal with no lymphadenopathy, hepatosplenomegaly, or skin lesions. CBC showed WBC 24.5 $\times$ 10^9/L with segmented neutrophils 10%, lymphocytes 5%, monocytes 2%, eosinophils 1%, basophils 1%, abnormal lymphocytes 81%, hemoglobin 12.0 g/dL, and platelets 210 $\times$ 10^9/L. Blood chemistry including lactate dehydrogenase and calcium were normal. Immunoglobin M was slightly elevated at 360 mg/dL, but other immunoglobulin classes were normal. Serum protein electrophoresis showed no monoclonal protein. Her hepatitis serology, including hepatitis B antigen and hepatitis C antibodies, was negative. Human T-cell lymphotropic virus-I and HIV antibodies were also negative. Peripheral blood smear (Fig 1) showed abnormal lymphocytes that were small and had indented and irregular nuclei with condensed chromatin and no apparent nucleolus. Cytoplasm was basophilic and lacked granulations. Bone marrow was hypercellular with diffuse infiltration by these same abnormal lymphocytes (Fig 2). Immunophenotype analysis (Fig 3) of peripheral blood revealed the abnormal lymphocytes were $CD1^-$, $CD2^+$, $CD3^+$, $CD4^-$, $CD5^+$, $CD7^+$, $CD8^+$, $CD10^-$, $CD16^-$, $CD19^-$, $CD20^-$, $CD22^-$, $CD23^-$, $CD25^-$, $CD30^-$, $CD34^-$, $CD38^{dim\,1}$, $CD45^1$, $CD56^-$, $CD57^-$, sIg^-, $TCR\alpha\beta^+$, $TCR\delta\gamma^-$, and TdT^-. Southern blot analysis for TCR-Cβ1 showed rearranged bands, suggesting a clonal process of disease (Fig 4). No metaphase cells for cytogenetic analysis were obtained in unstimulated culture of peripheral blood. Cytogenetic study with phytohemagglutinin stimulation showed 42, X, -X, add(6)(p25), add(7)(q36), I(8)(q10), −11, add(12)(p13), +13, −14, −15, −15, −17, add(19)(q13.4), add(20)(q13.3), −22, +mar2 in all nine cells analyzed (Fig 5). A diagnosis of $CD8^+$ T-cell prolymphocytic leukemia (T-PLL) was made. She developed progressive abnormal lymphocytosis, liver function test abnormalities, cervical lymphadenopathy, and erythematous skin lesions 3 months after diagnosis. She was

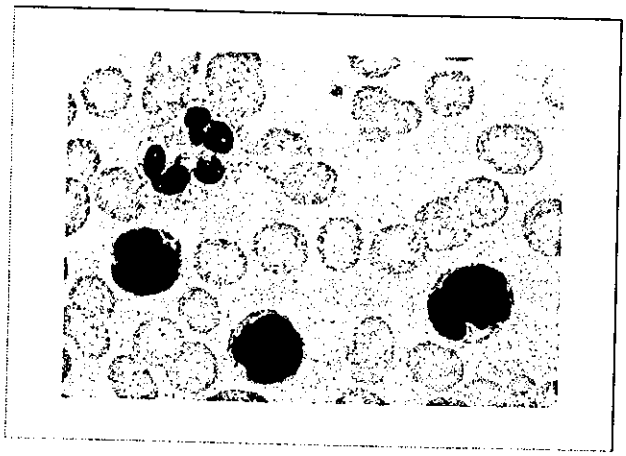

Fig 1.

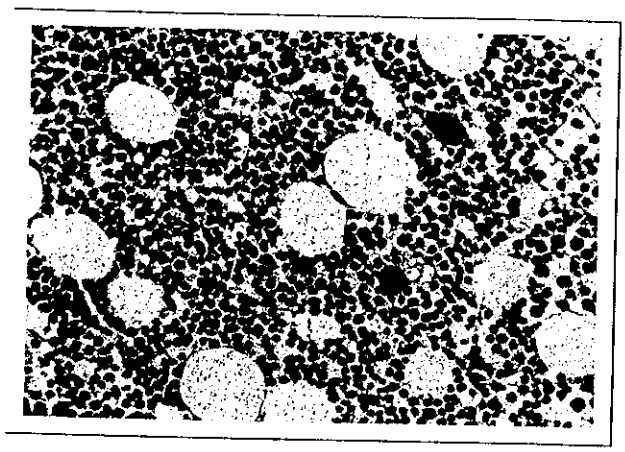

Fig 2.

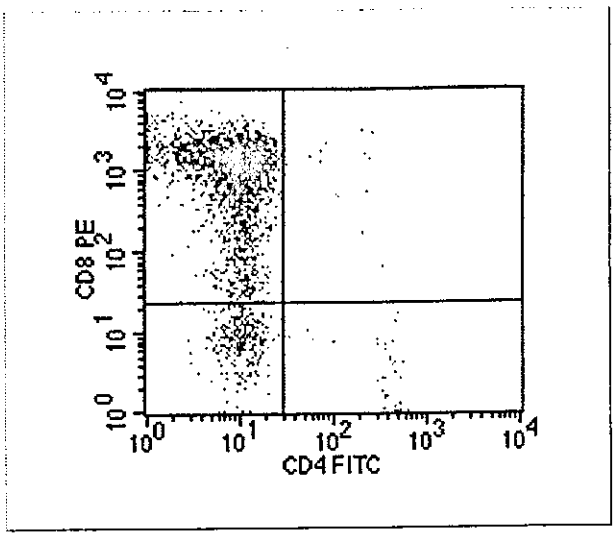

Fig 3.

treated with two courses of deoxycoformycin without any response. Therapy was changed to cyclophosphamide, doxorubicin, vincristine, and prednisone, resulting in resolution of liver function test abnormalities, decreased lymphadenopathy, and stable peripheral abnormal lymphocyte counts. She is awaiting an unrelated allogeneic bone marrow transplantation.

The differential diagnosis of increased abnormal T cells in the peripheral blood includes adult T-cell leukemia (ATL), leukemic phase of cutaneous T-cell lymphoma, large granular lymphocyte (T-LGL) leukemia and T-PLL. ATL was ruled out because of the negative serology for human T-cell lymphotropic virus-1 and the fact that most ATL are $CD4^+$ $CD8^-$. Cutaneous T-cell lymphoma was highly unlikely because of absence preceding cutaneous lesions. $CD3^+$ T-LGL leukemia is ruled out by lack of increased large granular lymphocytes with $CD16^+$ $CD57^+$ phenotype [1]. Additionally, patients with $CD3^+$ T-LGL leukemia present with neutropenia, anemia, and splenomegaly.

A new variant of T-cell chronic lymphocytic leukemia with $CD8^+$ phenotype was described in 1987 [2]. T-cell chronic lymphocytic leukemia is now reclassified as T-PLL according to the WHO/revised form of European-American Classification of lymphoid neoplasms classification for lymphoid malignancies because of aggressive clinical behavior [3]. It represents approximately 30% of T-cell leukemias with a mature phenotype. Clinical features of T-PLL include occurrence in older patients, hepatosplenomegaly, lymphadenopathy, skin lesions, leukocytosis, anemia, and thrombocytopenia [4]. The majority of cases are $CD4^+$ $CD8^-$; however, approximately 10% of T-PLL are $CD4^-$

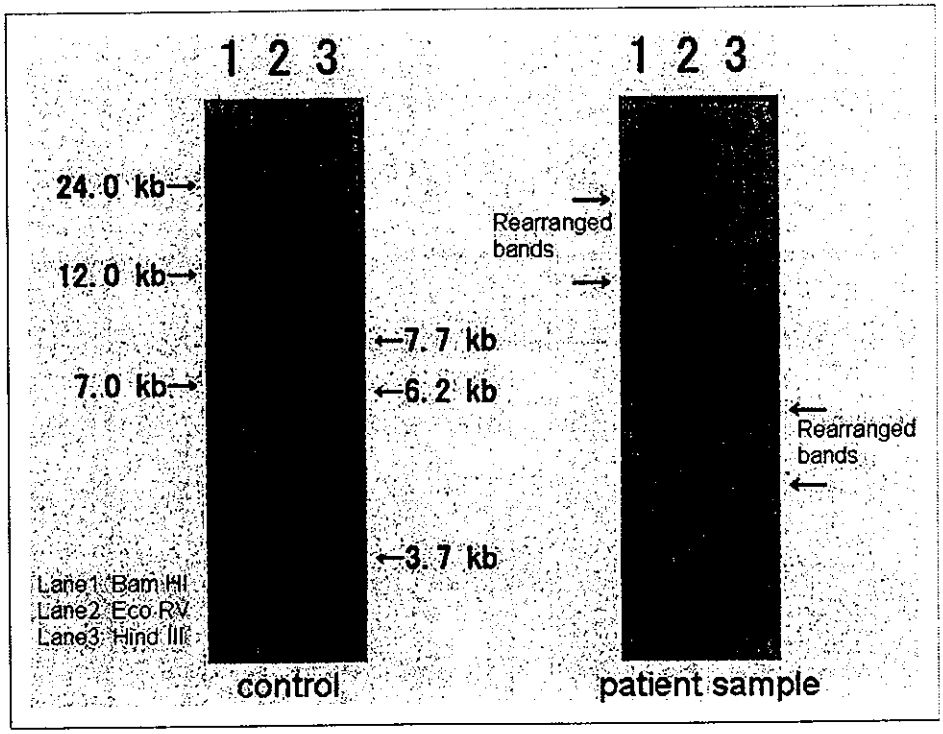

Fig 4.

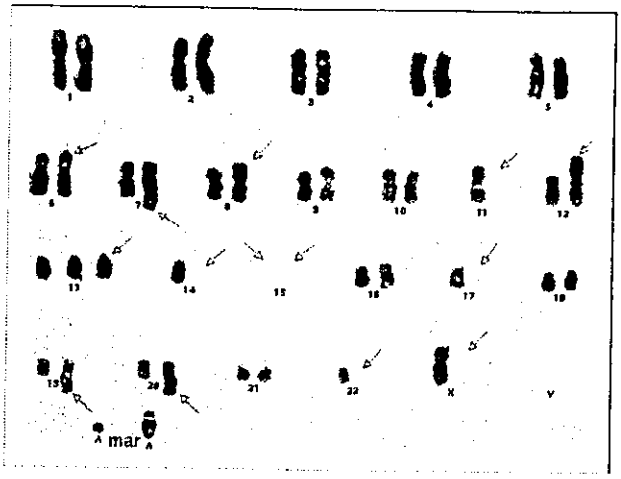

Fig 5.

$CD8^+$ [4,5]. Although no pathognomonic cytogenetic abnormalities have been identified, many cases show abnormalities involving chromosome 14 at bands q11 and q32 [4-8]. The clinical course is aggressive and tends to be resistant to chemotherapy. Median survival is approximately 1 year. Our case fulfills the clinical, morphologic, and immunophynotypic criteria for $CD8^+$ T-PLL with unusual cytogenetic abnormalities. It is important to recognize T-PLL because it has a more aggressive clinical course than mature T-cell leukemias.

Hikaru Nakajima, Masayuki Oki, and Kiyoshi Ando
Division of Hematology/Medical Oncology, Departments of Medicine
Tokai University School of Medicine, Isehara, Japan

Authors' Disclosures of Potential Conflicts of Interest

The authors indicated no potential conflicts of interest.

REFERENCES

1. Loughran TP Jr: Clonal diseases of large granular lymphocytes. Blood 82:1-14, 1993
2. Hui PK, Feller AC, Pileri S, et al: New aggressive variant of suppressor/cytotoxic T-CLL. Am J Clin Pathol 87:55-59, 1987
3. Harris NL, Jaffe ES, Stein H, et al: A revised European-American classification of lymphoid neoplasms: A proposal from the International Lymphoma Study Group. Blood 84:1361-1392, 1994
4. Matutes E, Brito-Babapulle V, Swansbury J, et al: Clinical and laboratory features of 78 cases of T-prolymphocytic leukemia. Blood 78:3269-3274, 1991
5. Matutes E, Catovsky D: Mature T-cell leukemias and leukemia/lymphoma syndromes. Review of our experience in 175 cases. Leuk Lymphoma 4:81-91, 1991
6. Heinonen K, Mahlamaki E, Hamalainen E, et al: Multiple karyotypic abnormalities in three cases of small cell variant of T-cell prolymphocytic leukemia. Cancer Genet Cytogenet 78:28-35, 1994
7. Brito-Babapulle V, Maljaie SH, Matutes E, et al: Relationship of T leukaemias with cerebriform nuclei to T-prolymphocytic leukaemia: A cytogenetic analysis with in situ hybridization. Br J Haematol 96:724-732, 1997
8. Brito-Babapulle V, Pomfret M, Matutes E, et al: Cytogenetic studies on prolymphocytic leukemia. II. T cell prolymphocytic leukemia Blood 70:926-931, 1987

DOI: 10.1200/JCO.2004.03.060